Chapter 3

Synthesis, Characterization and Catalytic Application of Imidazolium-based Nickel Complex for C-S Cross-Coupling Reaction in Water

3.1 Introduction

Nickel catalysis has made tremendous advances in organic synthesis for the construction of small and complex molecules [1-2]. Nickel was first identified and isolated by the Swedish Chemist Baron Axel Frederich Cronstedt in 1751 [3]. Initially, nickel was thought to be of not much use, but later the demand increased intensely due to its remarkable properties such as hardness, corrosion resistance, cost-effectiveness, and recyclability. Mostly it is found in steels and metal alloys but is also used in the production of permanent magnets and batteries [4]. It is the extensively used element in metal-based catalyst and its first application as a hydrogenation catalyst led to the Nobel Prize in Chemistry in 1912 [5]. Later on, its catalytic applications were observed in several processes, such as steam reforming [6], hydrogenolysis [7], desulfurization [8], reductive amination [9], and methanation [10]. Regardless of the enormous success and broad applications of the Ni catalyst in industry, Ni metal and its salts as catalysts are still not able to fulfill the desired requirements *viz.* activity, selectivity, and stability for many organic transformations. Tremendous research efforts have been made to improve the properties of traditional nickel catalyst and several nickel complexes of phosphines [11], bipyridines [12], Schiff bases [13] and N-heterocyclic carbenes [14] are widely explored in organic synthesis. Nickel complexes are used as catalysts for several organic reactions due to low cost, high abundance, ease of synthesis, higher reactivity, excellent thermal, and air stability [15-16]. They are utilized in different organic reactions like alkane and alkene oxidation [17], alkynylation of trifluoromethyl ketones [18], hydrogenation of ketones [19], and cross-couplings [20], etc.

C-X (X = carbon, oxygen, nitrogen, sulfur) cross-coupled products are important synthetic intermediates in the biochemistry and pharmaceutical industry [21]. This includes DNA cleavage, stabilisation of peptides in proteins, drugs, flavours, combinatorial synthesis and in the design of rechargeable lithium batteries. The aromatic carbon-sulfur bond formation is an important synthetic organic transformation [22]. The ubiquitous distribution of organosulfur functionalities in nature and biological systems represents its essential role in the maintenance and growth of life [23-24]. Organosulfur motifs widely exist in natural bioactive products and synthetic drugs, which has led to their application in the pharmaceutical industry [25-26]. A number of drugs in therapeutic areas such as diabetes and inflammatory, immune, Alzheimer's, and Parkinson's diseases contain the organosulfur functionality. Few examples of drugs containing organosulfur unit, which are employed as anti-depressant [27], anti-

tumour [28], antibacterial [29], anti-inflammatory, MCF-6 growth inhibitor [30] and LFA-1/ICAM-1 inhibitor [31] are given in **Figure 3.1**.

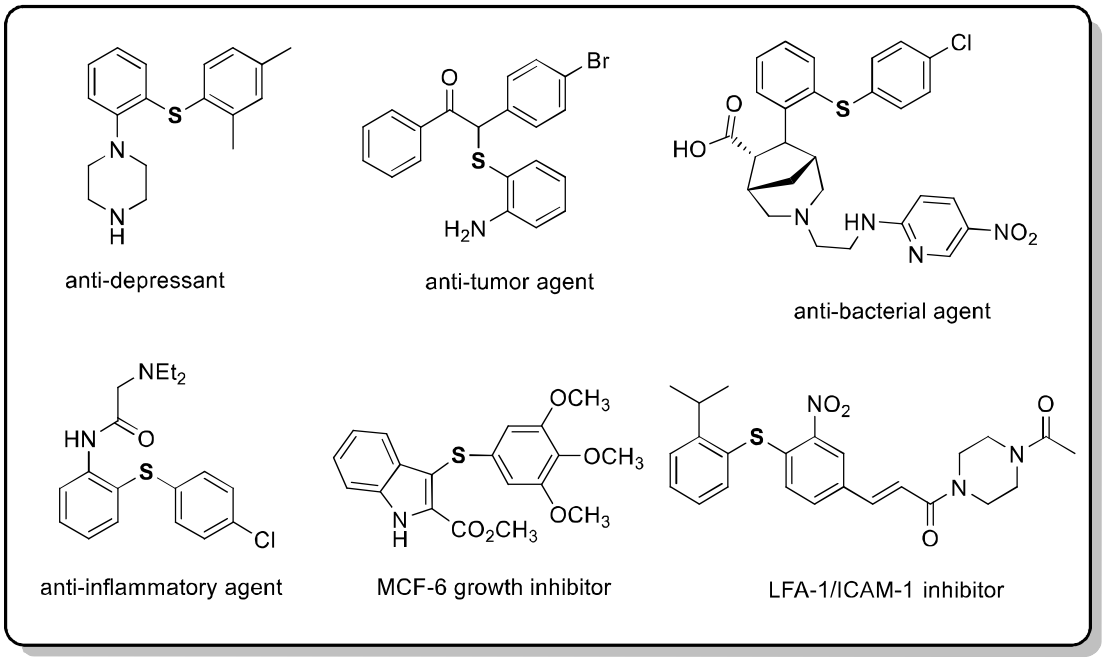

Figure 3.1 Selected examples of biologically active organosulfur derivatives

Organosulfur compounds can be synthesized by addition, substitution, and cross-coupling reactions. The traditional protocols for the synthesis of organosulfur compounds utilize transition metal-catalyzed cross-coupling of nucleophilic sulfur and electrophilic carbon source [32-33]. Among numerous reported procedures, palladium and copper-based catalysts are widely used under basic conditions. In addition, nickel, iron, indium, and other metal-based catalysts are also employed as effective catalysts for this transformation. However, many reports are available on palladium catalysts, whereas the applications of nickel and other transition metal complexes for C-S coupling are limited. Most of the palladium-catalyzed reactions are based on a Pd(0)/Pd(II) catalytic cycle. Similarly, Ni(0)/Ni(II) catalytic cycles are prevalent, but many transformations are also based on Ni(I)/Ni(III), Ni(0)/Ni(II)/Ni(I), Ni(II)/Ni(IV) or cycles in which Ni remains in the Ni(I) state for the entire catalytic cycle [34-35].

3.1.1 Nickel metal complexes for C-S cross-coupling reaction

Nickel complexes of Schiff base ligands have been extensively employed in various organic reactions including, polymerization [36], ring-opening of epoxides [37], Michael reactions

[38], epoxidation of olefins [39], nitroaldol condensation [40], transfer hydrogenation of ketones [41], etc., whereas a few reports are available for the C-S cross-coupling reactions.

Barman and coworkers reported *o*-aminophenol based Schiff base Ni(II) complex **1** (**Figure 3.2**) as a catalyst for the reaction of alkyl/aryl/benzyl chlorides with different thiophenol derivatives in presence of KOH in DMF. The aromatic chlorides having electron-withdrawing groups provided better yields in comparison with those having electron-donating groups. Benzyl chlorides were found to be most reactive and this protocol afforded a variety of C-S cross-coupled products in good to excellent yields [42]. Morales and coworkers reported eight fluorinated bis-imino Ni(II) NNN pincer complexes **2a-h** (**Figure 3.2**) for the thiolation of dialkyl/diaryl disulfides with iodobenzene derivatives using Zn metal as a reducing agent in DMF. From all the tested complexes, **2e** afforded higher yields of thiolated products [43]. They further extended the scope of reaction and obtained products in moderate yields from bromobenzene derivatives by changing temperature from 110 to 160 °C [44]. They also proposed an air and moisture stable phosphinite Ni(II) PCP pincer complex **3a** (**Figure 3.2**) for thiolation of iodobenzene with dialkyl/diaryl disulfides. Six derivatives of dialkyl/diaryl sulfides were prepared in excellent yields. They also proposed the mechanism for this transformation, which involved a 15-electron Ni(I) radical and a nickel thiolate intermediate [45]. Zhang *et al*. provided a mechanistic investigation of the sulfenylation reaction of aryl halides with thiophenol derivatives using complexes **3a-d** (**Figure 3.2**). Complexes **3b-d** exhibited less activity than **3a** due to the presence of sterically bulky groups at phosphorus atom which causes steric congestion at the nickel centre. $^{31}P\{^{1}H\}$ NMR spectroscopy suggested the formation of nickel thiolate complexes and participation of base in the generation of the active catalyst [46]. In another report, Morales and coworkers proposed a series of six SPS-Ni(II) pincer complexes **4a-f** (**Figure 3.2**) with different *para*-substituted triphenylphosphines. All complexes were tested for the sulfenylation reaction of iodobenzene and diphenyldisulfide with Zn as a reducing agent in DMF. Using complex **4a**, different dialkyl and diaryl disulfides on reaction with iodobenzene derivatives resulted in excellent yields of sulfides [47]. Serrano-Becerra *et al*. disclosed the synthesis and catalytic activity of phosphinite thiophosphinito POCSP-Ni(II) pincer complex **5** (**Figure 3.2**) for the C-S bond formation reaction.

The disulfide substrates with less steric hindrance was found to be more reactive than highly sterically hindered substrates [48].

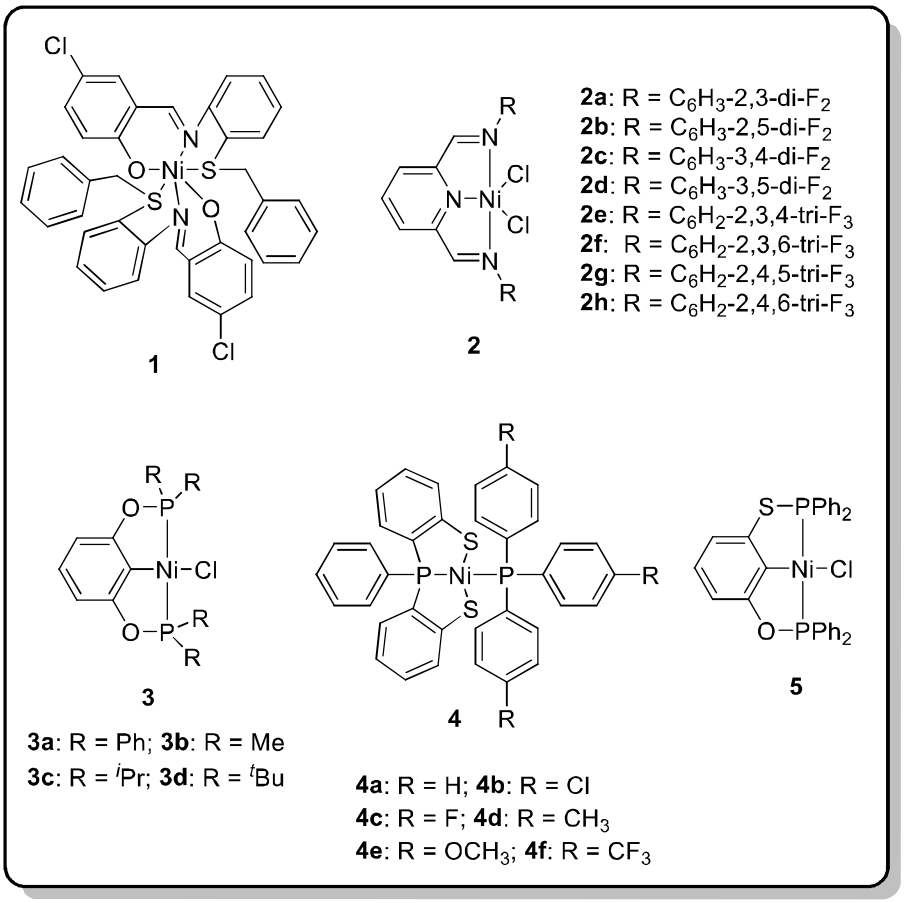

Figure 3.2 Schiff base (**1**) NNN (**2a-h**) PCP (**3a-d**) SPS (**4a-f**) and POCSP (**5**) pincer Ni(II) complexes

Venkanna *et al.* synthesized eight Ni(II) PNP pincer complexes **6a-h** (**Figure 3.3**) as precatalysts for the C-S cross-coupling reaction. They constructed a library of sulfenylated alkyl and aryl sulfides by using catalyst **6a** and studied the mechanism using all these precatalysts. With the help of ^{1}H and ^{31}P NMR spectroscopy and cyclic voltammetry techniques they proposed that Ni(I) generated by the reduction of Ni(II) in the presence of excess thiolate worked as an active catalyst [49]. Basauri-Molina *et al.* prepared a family of SCS and SNS pincer complexes **7a-c** and **8a-c** (**Figure 3.3**) and studied their effect on both the Suzuki-Miyaura and thioetherification C-S couplings under both conventional and microwave conditions.

They observed that Pd-SCS complexes were more efficient catalysts for Suzuki-Miyaura coupling and Ni-SNS for thioetherification C-S coupling [50].

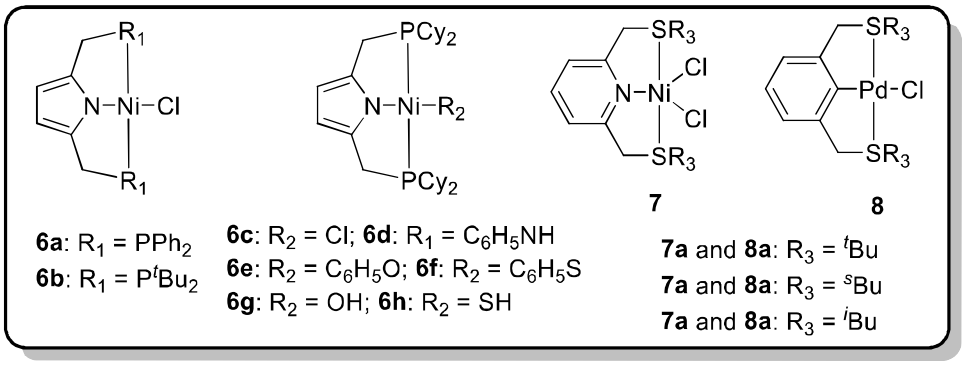

Figure 3.3 Ni(II) PNP (**6a-h**), SNS (**7a-c**) and Pd(II) SCS (**8a-c**) pincer complexes

Gehrtz *et al.* also reported the coupling of aliphatic and aromatic thiols with a variety of aromatic and heteroaromatic chlorides by using homogeneous nickel precatalysts **9a-b** (**Figure 3.4**). They used PhZnCl·LiCl and PhMgBr·LiCl as a stoichiometric base to generate *in situ* Mg or Zn thiolate with aryl chlorides. Precatalysts **9a** was found to be more active in comparison to **9b** [51].

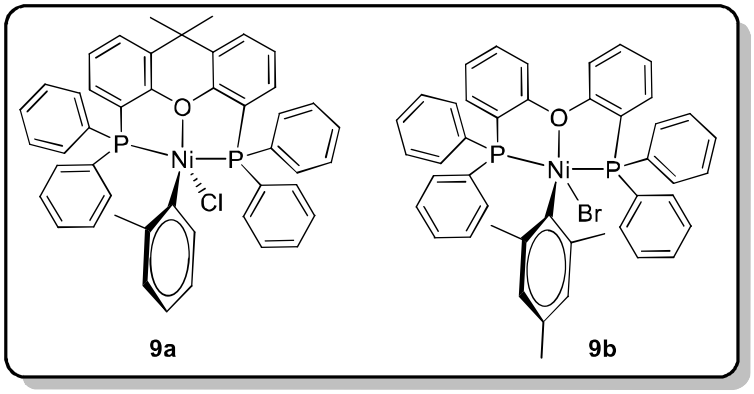

Figure 3.4 POP pincer (**9a-b**) Ni(II) complex

Zhang *et al*. disclosed the first series of NHC-based Ni catalysts and among them **10** (**Figure 3.5**) was found to be more active for sulfenylation reaction. It was found that the electronic and steric features of NHC ligand greatly affected the catalytic activities and the active specie involved was bis(NHC)-Ni(0) [52]. Further Iglesias *et al.* documented that complex **11** (**Figure 3.5**) for C-S cross-coupling between aryl thiols with iodo and bromobenzene derivatives afforded high yields of cross-coupled products at low catalyst loadings.[53] Martin *et al*. reported two complexes **12a** and **12b** (**Figure 3.5**) for the thiolation of aryl thiols with

aryl halides. Electron rich as well as electron-deficient aryl halides with electron-rich thiols provided high product yields [54]. Junquera *et al.* proposed two picolylimidazolidene based Ni-NHC complexes **13a** and **13b** (**Figure 3.5**) as efficient catalysts for sulfenylation reaction. Differently substituted aryl halides bearing electron-donating groups reacted efficiently with *p*-substituted aryl thiols having electron-donating or electron-withdrawing groups [55]. Working on supported catalysis, Yoon *et al.* documented the synthesis of magnetite/silica nanoparticle-supported NHC nickel catalyst **14** (**Figure 3.5**) for C-S bond formation. The reaction of thiophenols with aryl halides having electron-donating and electron-withdrawing substituents afforded aryl sulfides in excellent yields. This catalyst could be recovered by simple filtration and recycled up to three cycles [56]. Paul and coworkers developed a tetra-coordinated singlet diradical Ni(II) complex **15** (**Figure 3.5**) having two antiferromagnetically coupled one-electron oxidized redox non-innocent diamine type ligands for C-S bond formation. They proposed this methodology avoided high-energetic Ni(0)/Ni(II) or Ni(I)/Ni(III) redox steps in the catalytic cycle *via* synergistic participation of both nickel and the coordinated ligands during oxidative addition/reductive elimination steps [57].

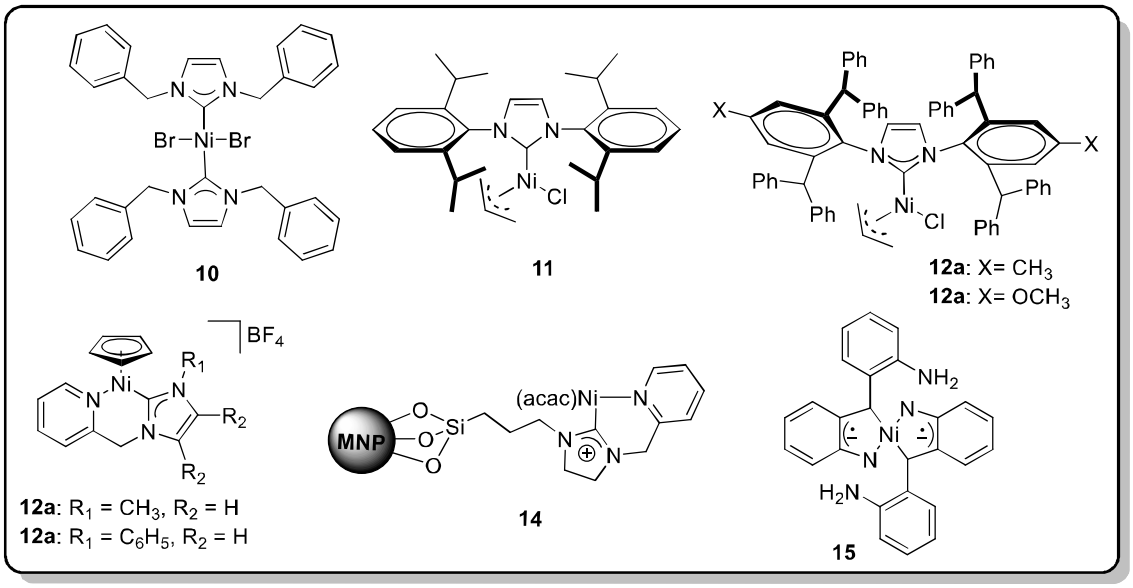

Figure 3.5 NHC (**10-14**) and diradical (**15**) Ni(II) complexes

Gupta and coworkers constructed two Ni(II) coordination polymers **16a** and **16b** based on two Co(III) metalloligands decorated with appended arylcarboxylate moieties (**Figure 3.6**). Both coordination polymers were used for the sulfenylation of aryl iodides with thiophenols and supported the exchange of coordinated water with the inclusion of iodine in the porous

network. Both **16a** and **16b** could be recycled up to five cycles without any loss in catalytic activity [58].

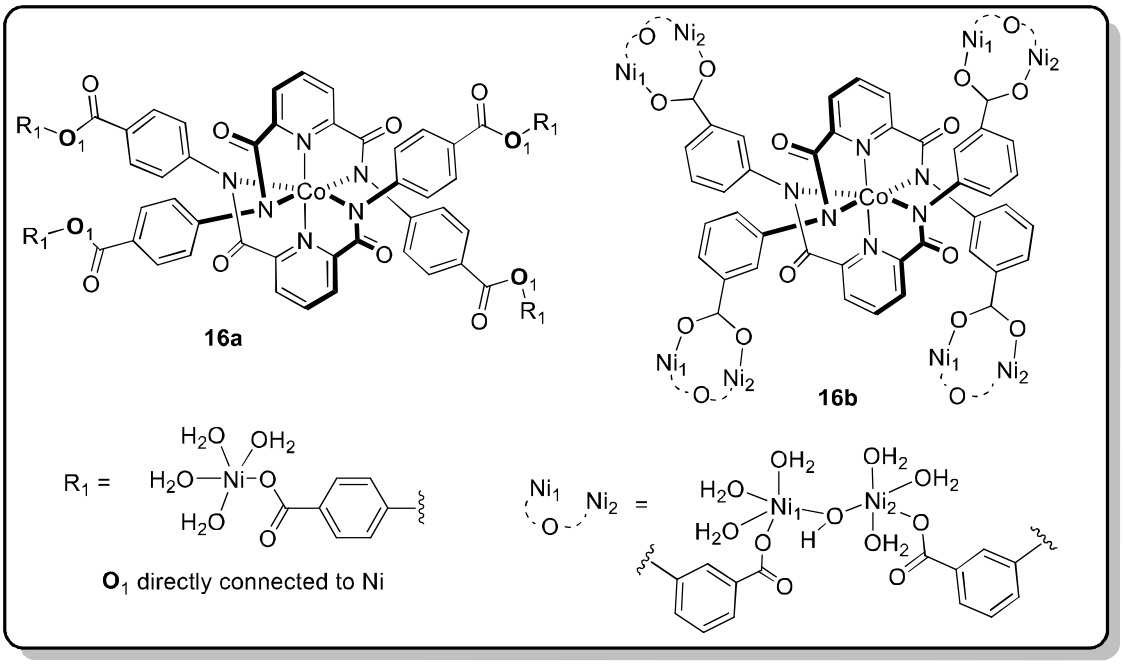

Figure 3.6 Ni (II) coordination polymers **16a-b**

3.1.2 Sulfonyl hydrazides as the sulfur source in C-S cross-coupling reaction

Traditional sulfenylating agents used for the C-S cross-coupling reaction are thiols, disulfides, thioamides, N-thioimides and 2-thiobenzamides [59-65]. But these are highly toxic, volatile, and foul-smelling sulfur sources and lead to serious environmental and health issues. The other limitations associated are catalyst deactivation through sulfur moieties, oxidative S-S coupling (disulfide formation), and difficult handling of the substrates [66-69]. Thus, in the search for efficient synthetic methodologies, another sulfur source, aryl/alkyl sulfonyl hydrazide, which is readily available, free of offensive odour and compatible with moisture, has been used. Many metal-based catalytic systems utilizing sulfonyl hydrazides have been reported to give the desired C-S coupled product in good yields.

Li *et al.* reported CuCl catalyzed regio- and stereoselective synthesis of sulfones and thioethers through N-S and/or S-O bond cleavage of sulfonyl hydrazides (**Scheme 3.1**). An array of alkenes bearing electron-withdrawing and electron-donating substituents provided the desired vinyl sulfones in moderate to high yields.

This method also afforded a variety of synthetically valuable aromatic and heteroaromatic thioether in good yields [70].

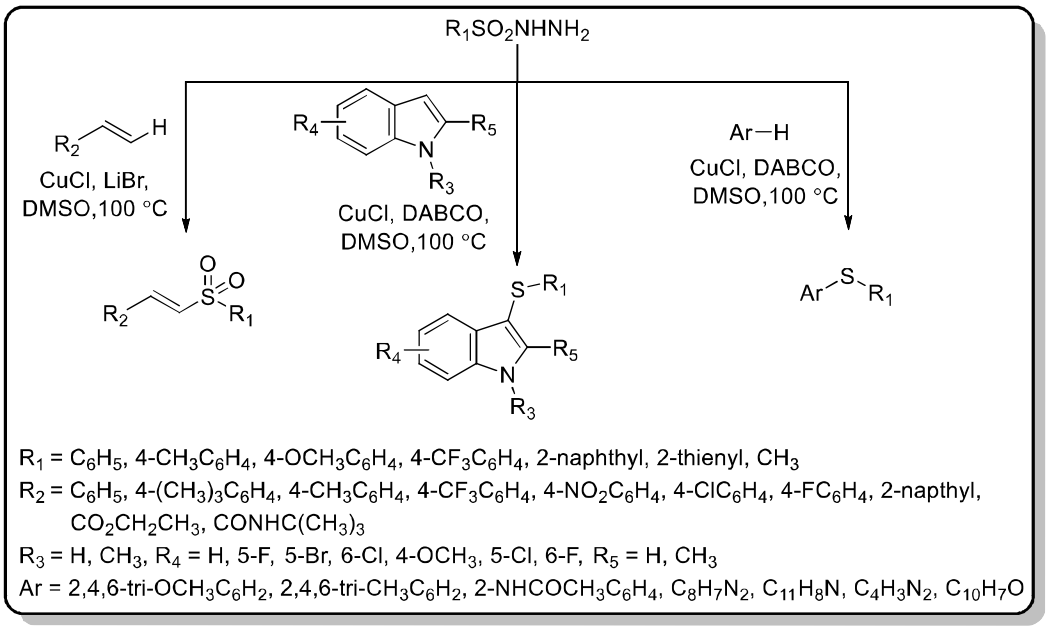

Scheme 3.1 Sulfenylation of alkenes, indoles, and arenes with sulfonyl hydrazides

Kumaraswamy and coworkers achieved aerobic dehydrogenative sulfenylation of H-phosphonates, H-phosphonites, and phosphine oxides with sulfonyl hydrazides catalyzed by a sub-stoichiometric amount of CuI (**Scheme 3.2**). The reaction progressed smoothly with aromatic as well as aliphatic sulfonyl hydrazides to afford the desired thiophosphate derivatives in good to high yields [71].

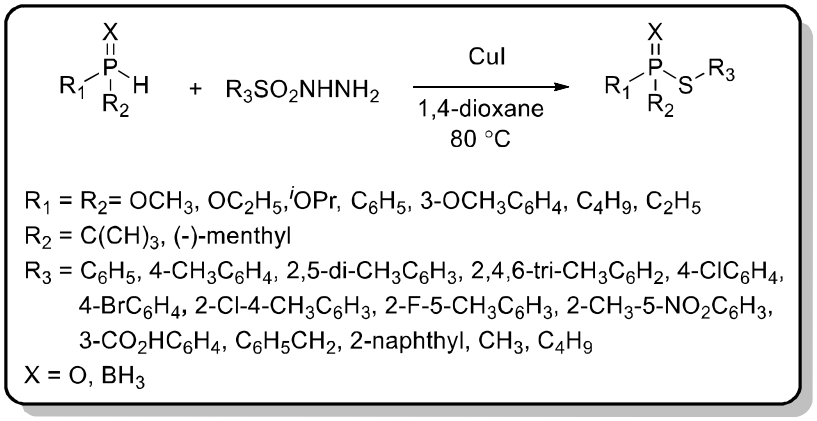

Scheme 3.2 Sulfenylation of H-phosphonates, H-phosphonites and phosphine oxides

Paul *et al*. disclosed a CuBr·Me_2S-catalyzed direct sulfenylation of 4-hydroxycoumarins and 4-hydroxyquinolinones to provide diverse 3-arylsulfanyl-4-hydroxycoumarins and 3-arylsulfanyl-4-hydroxyquinolinones in good yields (**Scheme 3.3**). This protocol involved the S-O, S-N bond cleavage of sulfonyl hydrazides and C-S cross-coupling reactions. Both 4-hydroxycoumarins and 4-hydroxyquinolinones substrates bearing electron-donating or electron-withdrawing groups provided good to high yields of desired products [72].

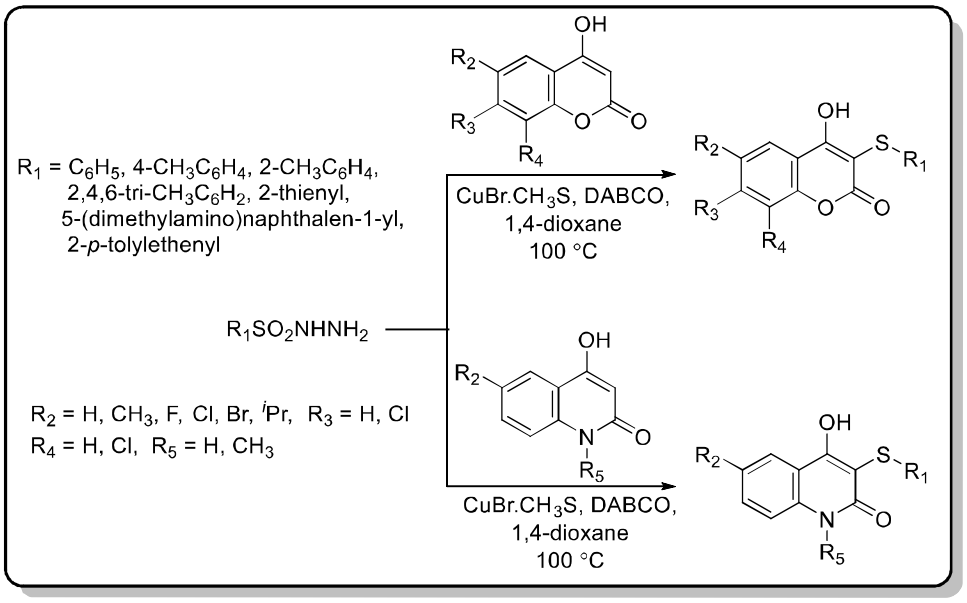

Scheme 3.3 Sulfenylation of 4-hydroxycoumarins and 4-hydroxyquinolinones

Yu *et al.* reported the synthesis of C5-sulfenylated 8-aminoquinolines using unprotected 8-aminoquinolines and sulfonyl hydrazides using CuI (**Scheme 3.4**). This protocol involved the direct reaction of NH_2-functionalized quinolines to afford the products containing a free NH_2 group without using any additional protection or deprotection step [73].

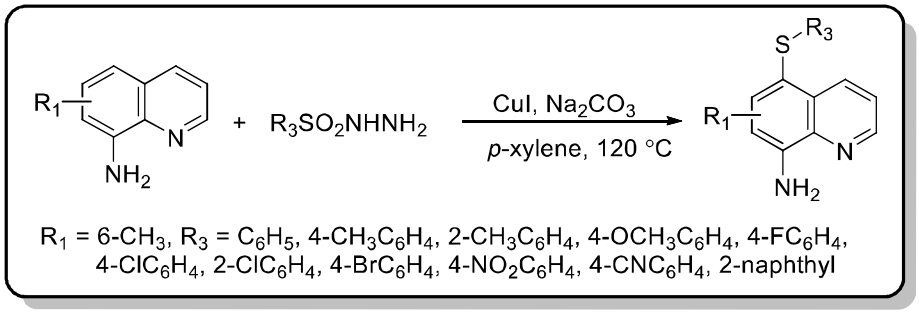

Scheme 3.4 C5-H sulfenylation of unprotected 8-aminoquinolines

Singh and coworkers reported microwave-assisted ionic liquid [DBU][HOAc] based CuI catalyzed synthesis of unsymmetrical sulfides using aryl/heteroaryl/benzyl halides (**Scheme 3.5**). The sulfonyl hydrazides with electron-donating groups and aryl halides with electron-withdrawing groups showed better yields. The reaction with aliphatic benzyl halides was also feasible without CuI, but product yields were low [74].

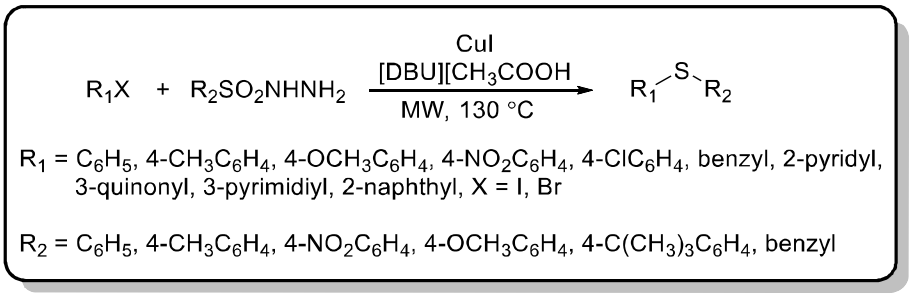

Scheme 3.5 C-S cross-coupling of aryl halides with sulfonyl hydrazides

Singh and coworkers proposed $NiCl_2 \cdot 6H_2O$/2,2′-bipyridine, DBU, and iodine-based cross-coupling of alkyl/aryl/heteroaryl boronic acids with alkyl/aryl sulfonyl hydrazides (**Scheme 3.6**). Both the coupling partners with electron-donating groups at the para-position provided excellent product yields whereas, the presence of electron-withdrawing groups reduced the product yields.[75] Wang *et al*. documented [$Cu(CH_3CN)_4BF_4$]/2,2′-bipyridine catalyzed sulfenylation of arylboronic acids with sulfonyl hydrazides (**Scheme 3.6**). The reaction well tolerated both electron-withdrawing and electron-donating groups either on aryl sulfonyl hydrazides or arylboronic acids. The reaction also worked well with alkylboronic acids but octyl sulfonyl hydrazide gave a complex mixture of products [76].

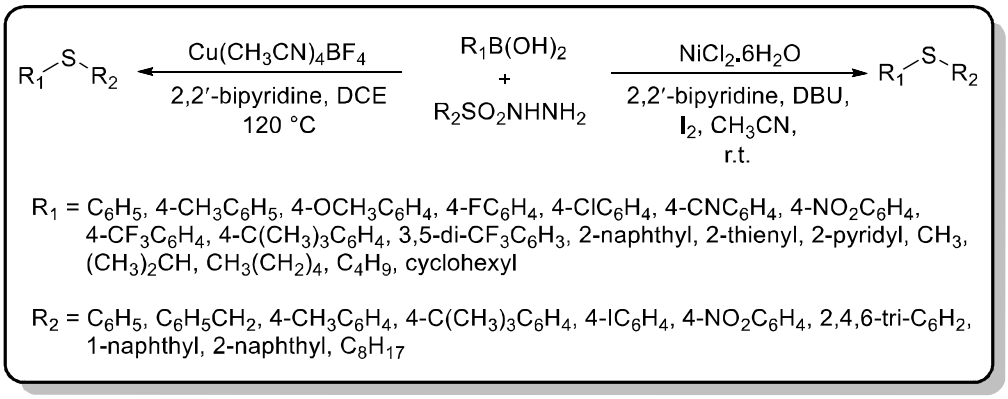

Scheme 3.6 Sulfenylation of boronic acids with sulfonyl hydrazides

Sun *et al*. disclosed an oxidative sulfenylation protocol for the formation of diverse sulfenyl amides in the presence of $Mn(OAc)_2$/DTBP catalyst system (**Scheme 3.7**). N-methyl amides worked as a solvent as well as an amide source in reaction. Sulfonyl hydrazine as a sulfur source in the presence of a manganese salt activated the sp^3 C-H bond of N-methyl amides through a free-radical pathway using DTBP [77].

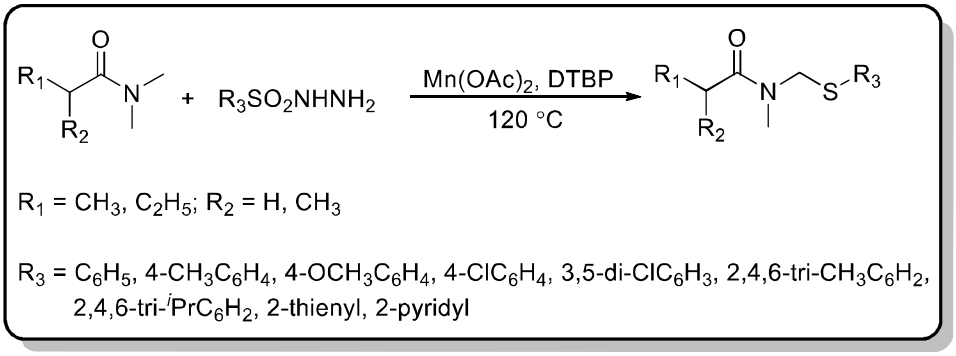

Scheme 3.7 Sulfenylation of N-methyl amides with sulfonyl hydrazides

Xu *et al.* achieved regioselective hydroxysulfenylation of unactivated C=C double bonds of N-allylsulfonamides with sulfonyl hydrazides using $FeBr_3$ and $Na_2S_2O_8$ as the oxidant in 1,4-dioxane-H_2O to provide a variety of β-hydroxysulfides in moderate to good yields (**Scheme 3.8**). The mechanism studies suggested that reaction in dry 1,4-dioxane or 1,4-dioxane/ethanol solvents gave the product in reduced yields, suggesting that H_2O played a role in the reaction [78].

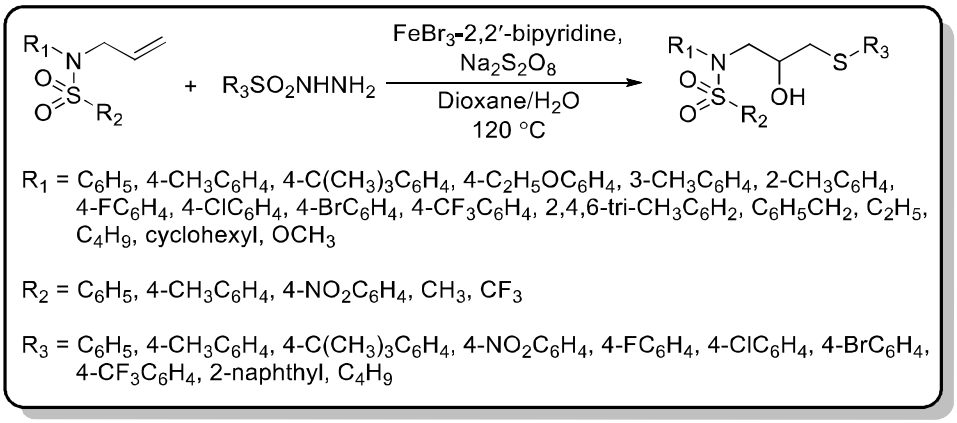

Scheme 3.8 Regioselective hydroxysulfenylation of N-allylsulfonamides

Kumar and coworkers reported the regioselective sulfenylation of indoles with aryl sulfonyl hydrazides using $CeCl_3 \cdot 7H_2O$-NaI in ethanol (**Scheme 3.9**). This method involved the breaking of S-O and S-N bonds and the formation of a C-S bond. The indoles containing

electron-donating group reacted faster as compared to the indoles with electron-withdrawing groups. This method worked equally well with the electron-deficient and electron-rich hydrazides under the given conditions [79].

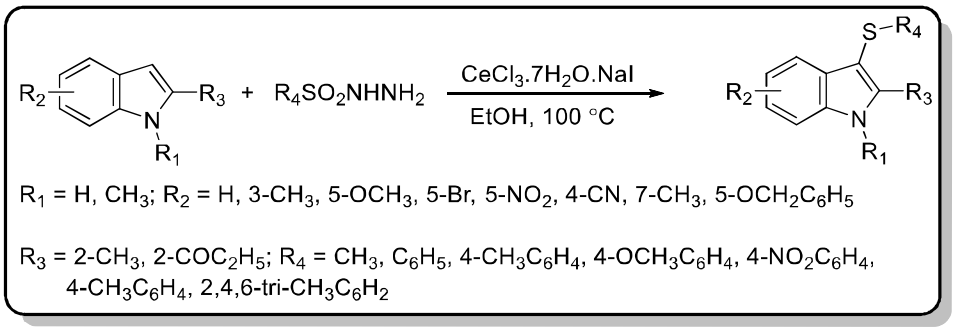

Scheme 3.9 Regioselective sulfenylation of indoles with sulfonyl hydrazides

The methodologies for C-S bond formation are associated with certain drawbacks *viz.* harsh reaction conditions, tedious workup, toxic organic solvents, etc. Therefore, it is a challenging task for synthetic chemists to overcome these limitations by simplifying the reaction condition and waste minimization. The catalytic reactions in water have gained importance over the last few decades because it is readily available, non-toxic, and non-flammable solvent for several organic transformation reactions involving metal catalyst [80]. Moreover, microwave synthesis has gained much attention due to its unique features including shorter reaction time, enhanced reaction rate, adjustable activation parameters, and excellent atom efficiency [81]. Therefore, a water-soluble imidazolium-based nickel catalyst for the C-S cross-coupling reaction is developed. Reaction under microwave irradiation, using water as a solvent, employing sulfonyl hydrazide as a sulfur source, and recycling of catalyst are the highlighting features of this protocol.

3.2 Results and Discussion

3.2.1 Synthesis and characterization of $L1H_2$ and L1Ni

Imidazolium-based aldehyde **ImA** was synthesized based on our previously reported methods [82-83]. Initially **ImA** was treated with ethylenediamine to give ligand $\mathbf{L1H_2}$. Further $\mathbf{L1H_2}$ reacted with $Ni(OAc)_2.4H_2O$ and gave corresponding Ni(II) complex **L1Ni** in 95% yield (**Scheme 3.10**). Both $\mathbf{L1H_2}$ and **L1Ni** were stable in air and completely soluble in highly polar solvents (DMF, DMSO, MeOH, EtOH, water, etc.). In the solid-state, $\mathbf{L1H_2}$ and **L1Ni** were obtained respectively as bright yellow and brown coloured solids. The structures of both $\mathbf{L1H_2}$ and **L1Ni** were well established using FT-IR, UV-visible, ^1H and ^{13}C NMR spectroscopy and

mass spectrometry. Several trials failed to yield suitable crystals of both **L1H$_2$** and **L1Ni** for single-crystal XRD.

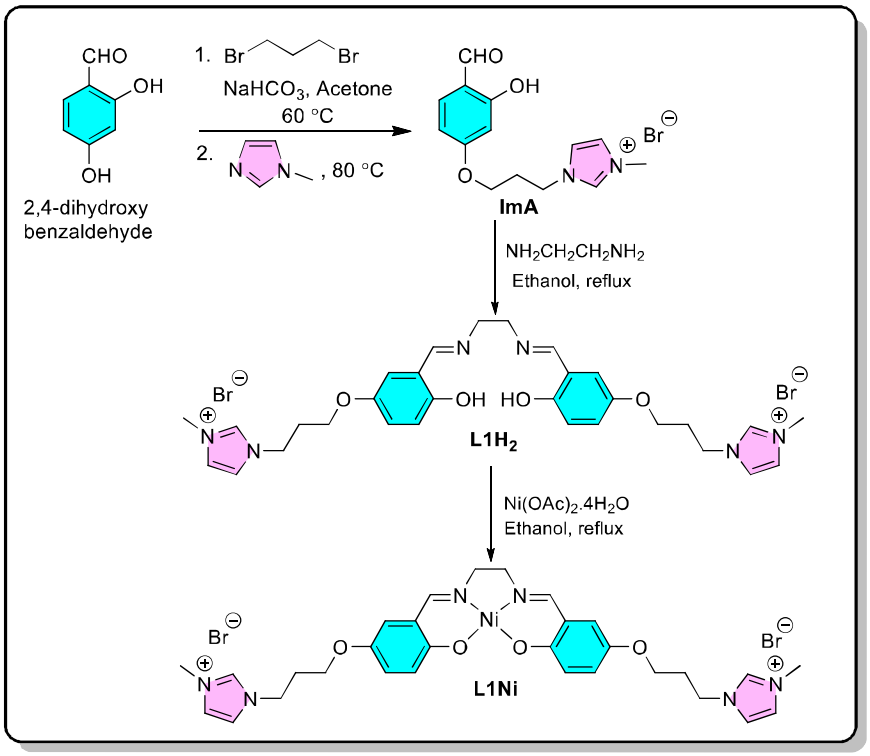

Scheme 3.10 Synthesis of ligand **L1H$_2$** and complex **L1Ni**

In the IR spectra (**Figure 3.7**), a peak at 1623 cm^{-1} due to *ν*(C=N) stretching in the spectrum of **L1H$_2$** shifted towards a lower frequency (1605 cm^{-1}) in the spectrum of **L1Ni**, which suggested coordination through the two azomethine groups.

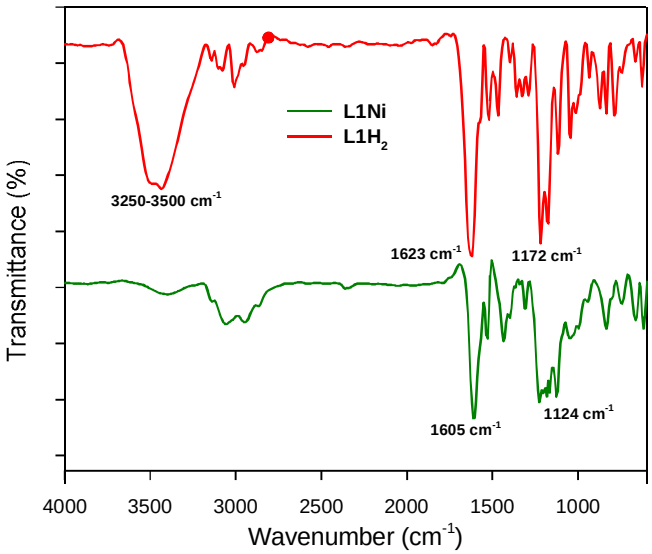

Figure 3.7 IR Spectra of **L1H$_2$** and **L1Ni**

In the spectrum of **L1H$_2$**, a broad band due to the intra-molecular hydrogen-bonded O-H group was observed at 3250-3500 cm^{-1}, this disappeared in **L1Ni** due to deprotonation upon complexation. The phenolic C-O stretching peak observed at 1172 cm^{-1} in **L1H$_2$** shifted to 1124 cm^{-1} in **L1Ni** further confirmed the coordination [84-85].The UV-visible spectral studies were performed in DMSO solvent (**Figure 3.8a**). For **L1H$_2$**, two intense absorption bands appeared at 278 nm and 308 nm due to the excitation of the π-electrons of the aromatic ring and a third band at 393 nm was attributed to the n-π^* transition of the C=N groups. For **L1Ni**, along with these three absorption bands, a band at 438 nm appeared due to the charge transfer transitions and a characteristic broad band with weak intensity (540-560 nm) due to *d-d* transitions. This broad band was further confirmed in the solid-state UV-visible spectra and its presence suggested the formation of a square planar complex (**Figure 3.8b)** [86-87].

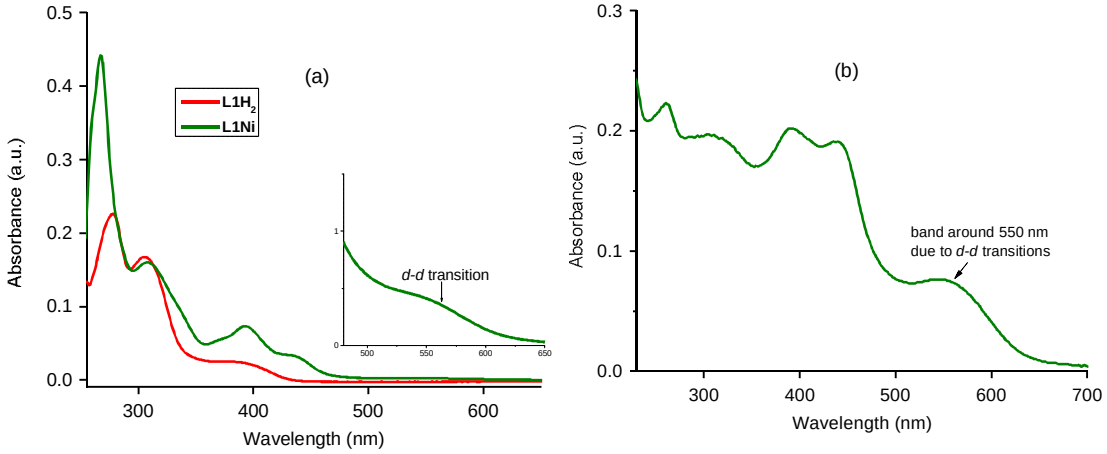

Figure 3.8 UV-visible spectra of (**a**) **L1H$_2$** and **L1Ni** in DMSO (10^{-5} M) (**b**) **L1Ni** in solid-state

The ^{1}H NMR spectrum of **L1H$_2$** showed resonance signals at δ 8.45 assigned to the azomethine protons and a downfield singlet at 13.79 ppm due to the phenolic -OH protons (**Figure 3.9**). The shift of the H-C=N- protons to δ 7.81 and the absence of -OH signals in **L1Ni** confirmed the bonding of oxygen and nitrogen with the metal ion. In the ^{1}H NMR spectrum of **L1Ni**, the presence of only one sharp singlet for the -CH=N proton indicated equivalent magnetic environment for both protons and planar arrangement of the ligand around the nickel ion (**Figure 3.10**). Also, the absence of any other proton signal confirmed the proposed environment around the nickel centre.

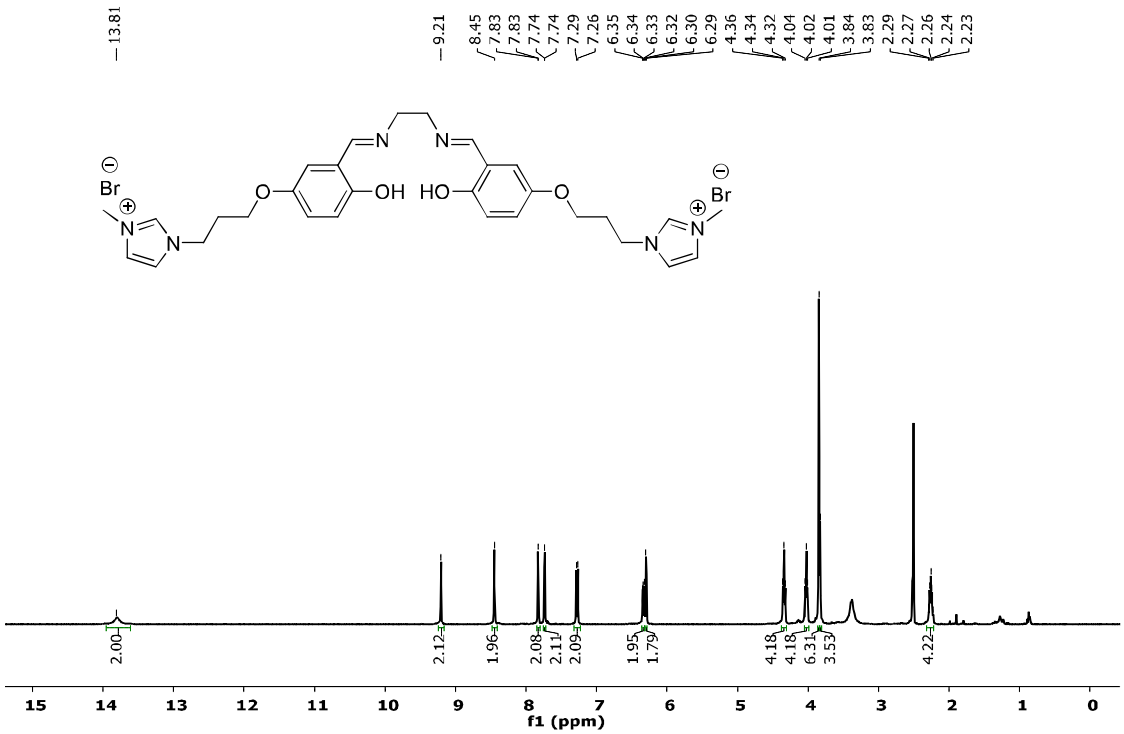

Figure 3.9 ^{1}H Spectrum of **L1H$_2$** (DMSO-d_6)

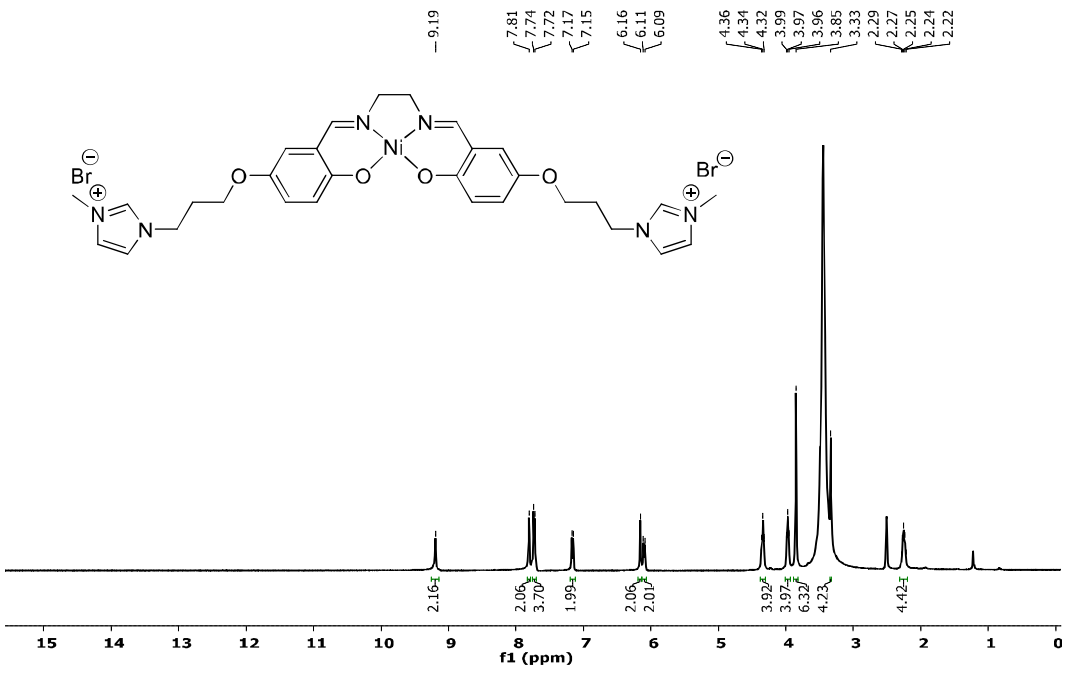

Figure 3.10 ^{1}H NMR Spectrum of **L1Ni** (DMSO-d_6)

The ^{13}C NMR spectrum of **L1H$_2$** showed a strong NMR signal at δ 163.2, which may be assigned to the azomethine carbon, and on coordination with nickel metal, it shifted downfield

to δ 165.8 ppm. All the other ^{13}C NMR signals were in agreement with the proposed structure (**Figure 3.11** and **Figure 3.12**) [88-89].

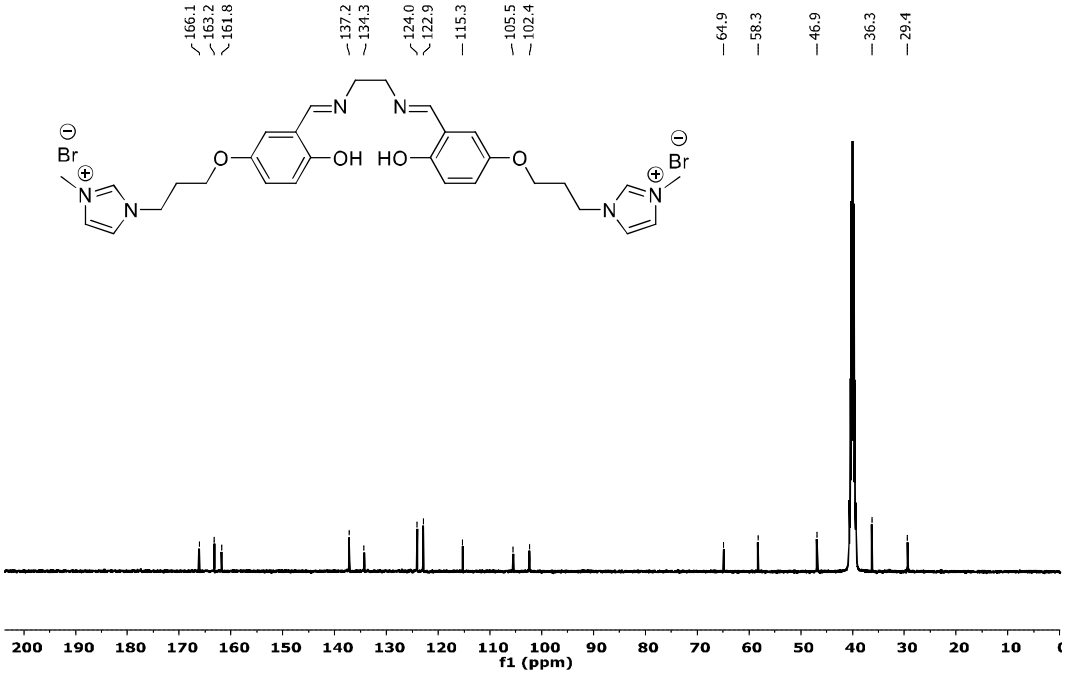

Figure 3.11 ^{13}C NMR Spectrum of **L1H$_2$** (DMSO-d_6)

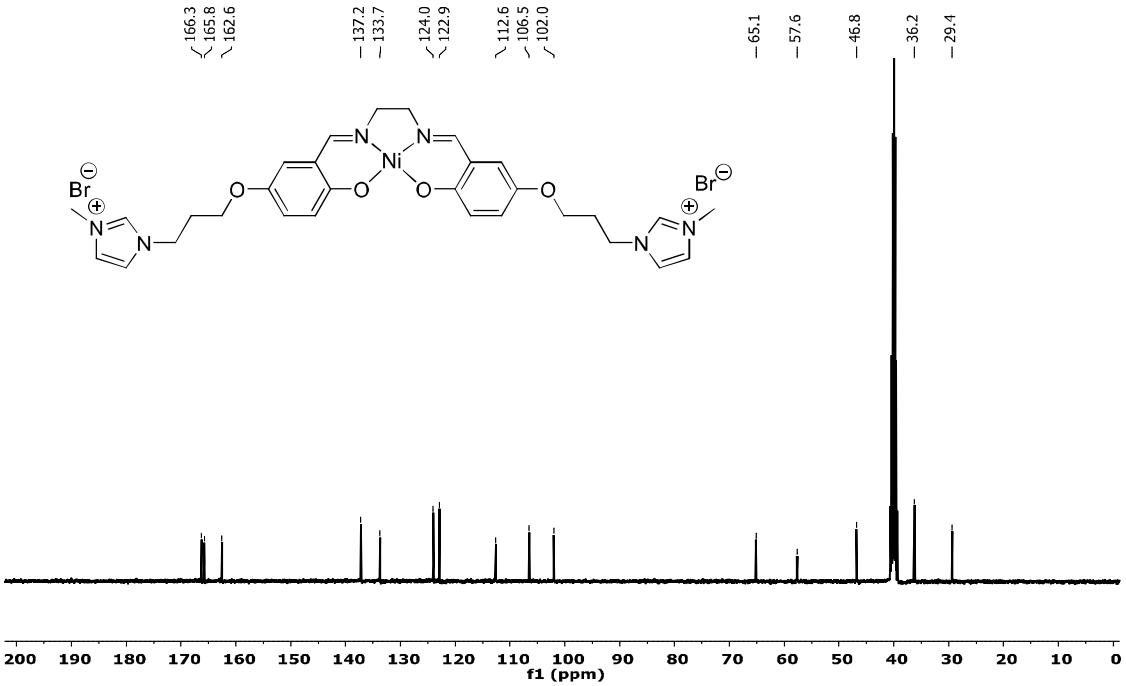

Figure 3.12 ^{13}C NMR Spectrum of **L1Ni** (DMSO-d_6)

The high-resolution mass spectrum of **L1H$_2$** showed an *m/z* (*z* = 2) peak at 273.1483 (found) (273.1472 calculated), which corresponds to [**L1H$_2$** - 2Br]$^{2+}$ (**Figure 3.13**) and for **L1Ni**, an

m/z peak at 301.1069 (found) (301.1071 calculated) due to [**L1Ni** - 2Br]$^{2+}$ (**Figure 3.14**). These peaks further supported the same structures and absence of other coordinating groups around the metal ion.

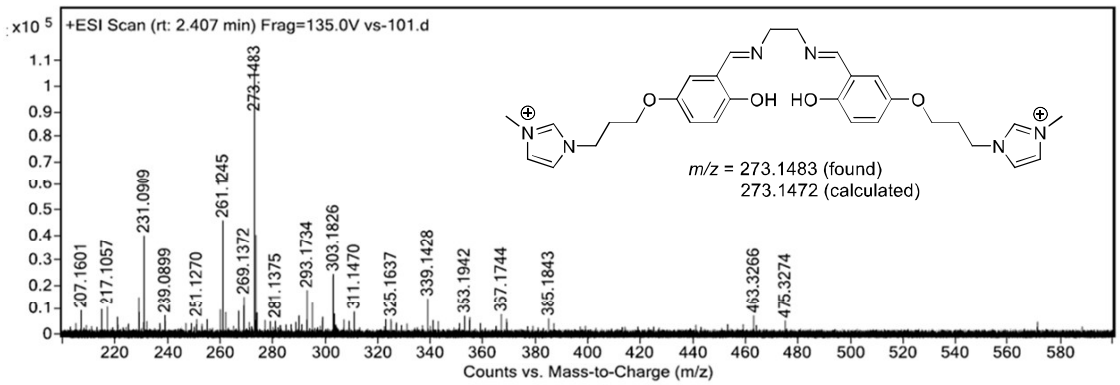

Figure 3.13 HRMS of **L1H$_2$**

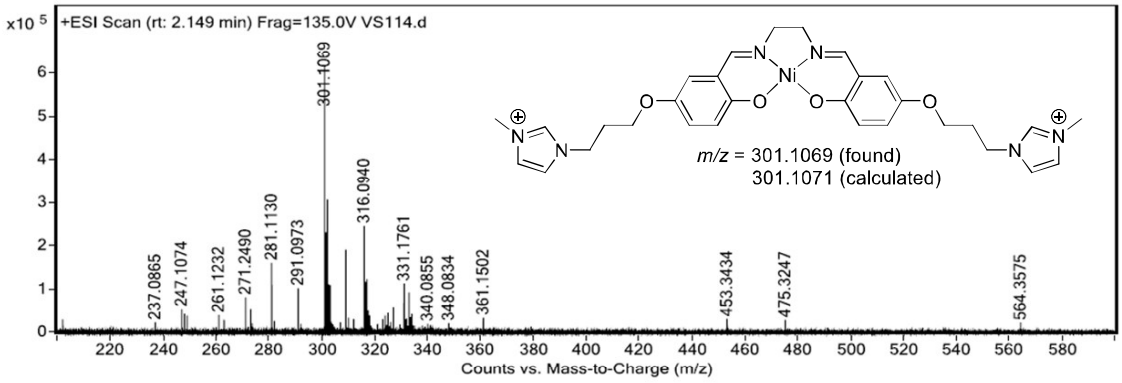

Figure 3.14 HRMS of **L1Ni**

3.2.2 Catalytic application of L1Ni in C-S cross-coupling reaction

After successful synthesis and characterization of **L1H$_2$** and **L1Ni**, the catalytic efficiency of **L1Ni** for the C-S cross-coupling reaction was explored. Initially, the C-S cross-coupling of iodobenzene **17a** and *p*-tolylsulfonyl hydrazide **18b** in the presence of catalyst **L1Ni** was selected as the model substrates for the optimization of the reaction conditions. The influence of base, temperature, and catalyst loading was investigated to determine the most suitable conditions for this transformation (**Table 3.1**). Using water as a solvent, different organic and inorganic bases (3 equiv.) such as DBU, K_2CO_3, Cs_2CO_3, and NEt_3 along with 10 mol% of catalyst **L1Ni** at 120 °C temperature under microwave irradiation (MW) was investigated (**Table 3.1**, entries 1-4). Base K_2CO_3 and Cs_2CO_3 showed less conversion (**Table 3.1**, entries 2 and 3) whereas, by using DBU and NEt_3 the product yield was improved (**Table 3.1**, entries 1 and 4). In the case of NEt_3, similar product yields were observed at 2 equiv. and 3 equiv. of

the base at a catalyst loading of 5 mol% (**Table 3.1**, entries 5-6). No improvement in the product yield was observed at high (10 mol%) and low (4 mol%) catalyst loading (**Table 3.1**, entries 4 and 8). The lower yield of the product was observed at low (110 °C) and high (130 °C) temperature (**Table 3.1**, entries 9-10). Using $Ni(OAc)_2.4H_2O$ under standard reaction condition no product formation was observed (**Table 3.1**, entry 13).

Table 3.1 Optimization of the reaction conditions[a]

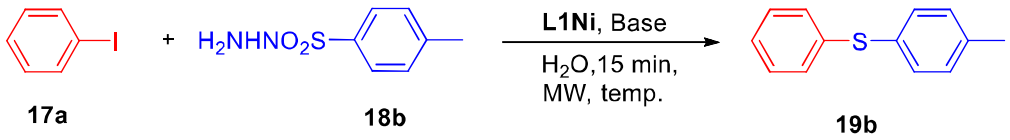

17a **18b** **19b**

Entry	Catalyst (mol %)	Base (equiv.)	T (°C)	Yield[b] (%)
1	**L1Ni** (10)	DBU (3)	120	60
2	**L1Ni** (10)	K_2CO_3 (3)	120	21
3	**L1Ni** (10)	Cs_2CO_3 (3)	120	23
4	**L1Ni** (10)	NEt_3 (3)	120	82
5	**L1Ni** (5)	NEt_3 (3)	120	86
6	**L1Ni** (5)	**NEt_3 (2)**	**120**	**86**
7	**L1Ni** (5)	NEt_3 (1)	120	40
8	**L1Ni** (5)	NEt_3 (2)	120	65
9	**L1Ni** (5)	NEt_3 (2)	130	53
10	**L1Ni** (5)	NEt_3 (2)	110	19
11	**L1Ni** (5)	NEt_3 (2)	120	-
12	**L1Ni** (5)	-	120	-
13	$Ni(OAc)_2.4H_2O$ (5)	NEt_3 (2)	120	-

[a]Reaction condition: **17a** (1 mmol), **18b** (2 mmol), water (3 ml).

[b]Isolated yield.

After having the optimized reaction conditions in hand, the scope and versatility of this method were extended to the reaction of phenyl, *p*-tolyl, *p*-nitrophenyl, benzyl, *p-tert*-butylphenyl, and 2-naphthyl hydrazides with different aryl halides. A diverse range of unsymmetrical diaryl sulfides **19a-s** were obtained in moderate to good yields under MW for 15 min (**Table 3.2**). Both electron-donating and electron-withdrawing groups at different positions of the reactants were well tolerated during the reaction. The reactants having electron-donating groups at the para position provided good yields of diaryl sulfides (**Table 3.2**, entries **19b**, **19c**, **19b′**, **19g**,

and **19h**). Aryl halides derivatives with electron-withdrawing groups at the para position (**Table 3.2**, entries **19d′** and **19i′**) were more reactive than the similarly substituted sulfonyl hydrazides derivatives (**Table 3.2**, entries **19d** and **19i)**. Aryl halides bearing chloro and fluoro groups at the para position also provided satisfactory yields (**Table 3.2**, entries **19f** and **19k**). The less reactive *o*-nitro and *o*-amino aryl iodide (**Table 3.2**, entries **19e** and **19l**) also reacted under these reaction conditions.

Table 3.2 Substrate scope for sulfenylation reaction using L1Ni[a, b]

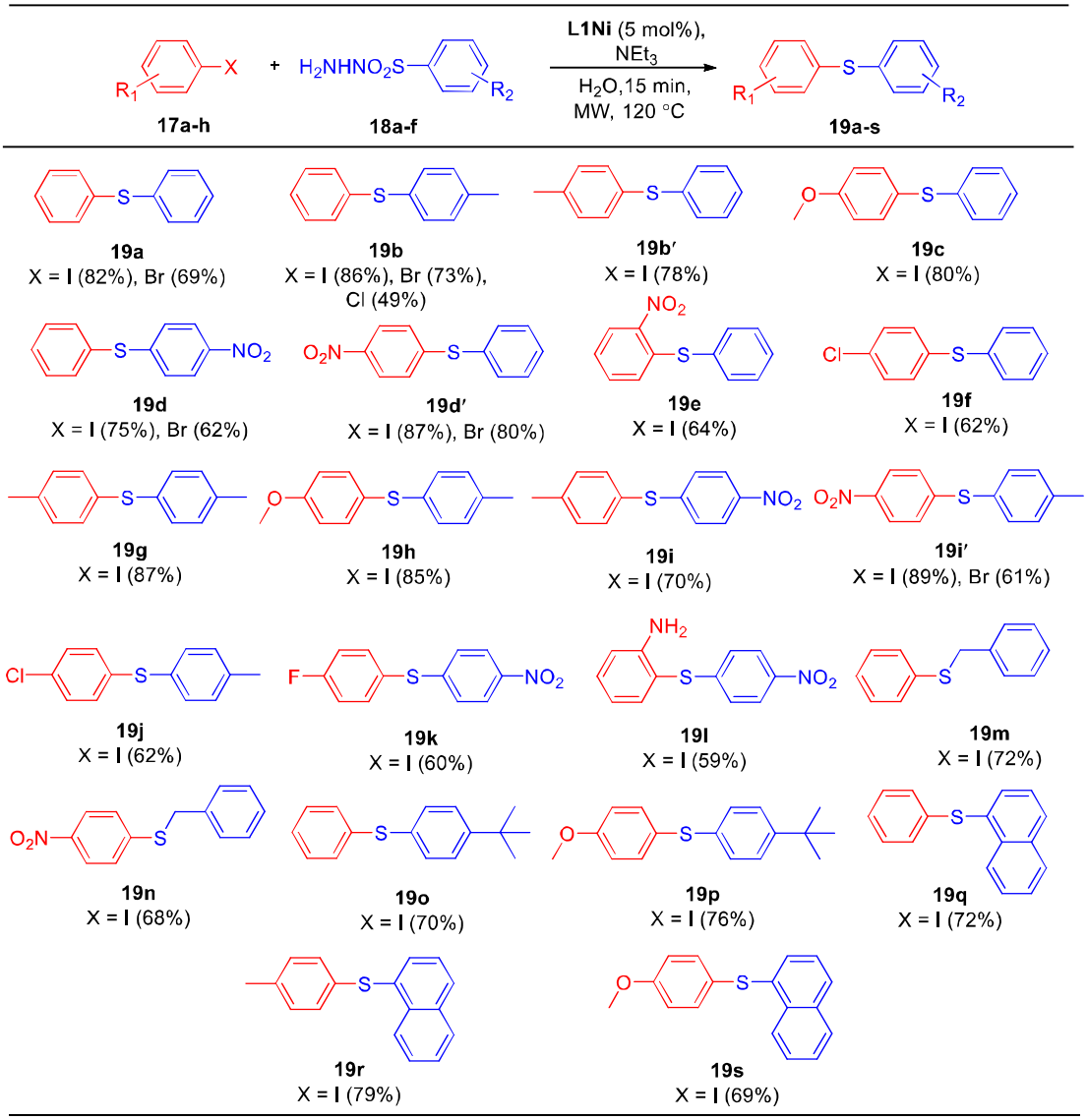

[a]Reaction condition: aryl halide (1 mmol), sulfonyl hydrazide (2 mmol), **L1Ni** (5 mol%), NEt_3 (2 equiv.), water (3 ml). [b]Isolated yield.

Additionally, sterically hindered and bulky sulfonyl hydrazides also reacted well to provide the desired thioethers (**Table 3.2**, entries **19o**, **19p**, **19q**, **19r,** and **19s**). The reaction was also

performed using other haloarenes. Only bromobenzene and *p*-nitrobromobenzene reacted (**Table 3.2**, entries **19b**, **19d** and **19d′**) and the trials failed for other derivatives of bromobenzene. In the case of chloroarenes only chlorobenzene reacted with *p*-tolylsulfonyl hydrazide and gave 49% product yield (**Table 3.2**, entry **19b**). All the synthesized compounds were isolated by column chromatography and characterized by ^{1}H and ^{13}C NMR spectroscopy. A representative ^{1}H and ^{13}C NMR spectrum depicted in **Figure 3.15** and **Figure 3.16** confirms the proposed structure of **19b**.

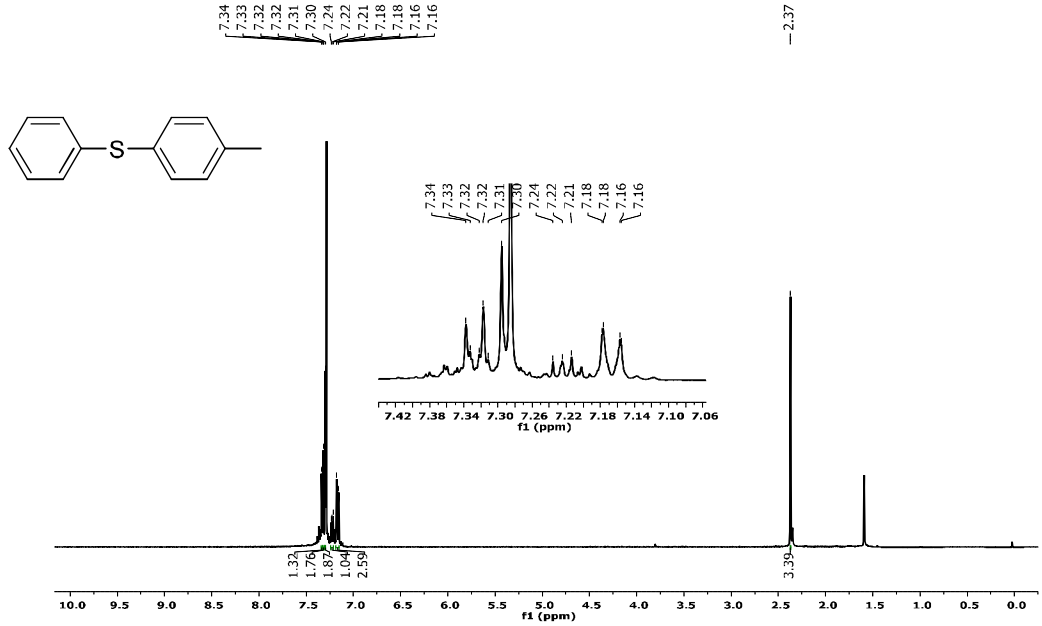

Figure 3.15 ^{1}H NMR Spectrum of **19b** ($CDCl_3$)

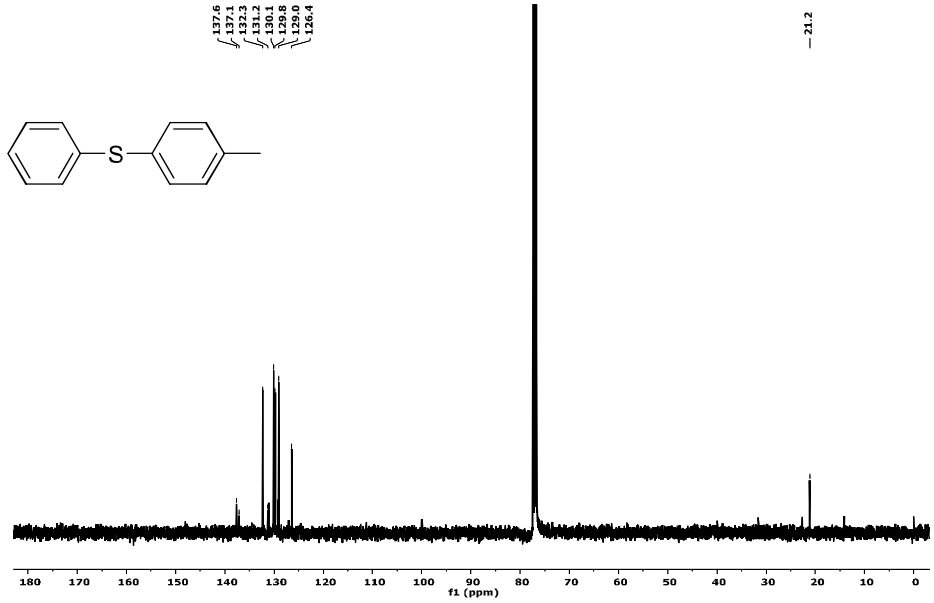

Figure 3.16 ^{13}C NMR Spectrum of **19b** ($CDCl_3$)

3.2.3 Recyclability of catalyst L1Ni

The reusability of the aqueous catalytic system is very important from practical and economic viewpoints. Therefore, a reusability test on **L1Ni** was performed, where the use of this water-soluble nickel catalytic system enabled the easy separation of the catalyst from the organic phase. After the completion of reaction, the product was extracted in ethyl acetate and the aqueous layer containing **L1Ni** was further charged with iodobenzene, sulfonyl hydrazide, and base for the second run. The same procedure was applied for the next consecutive cycles and the catalyst was recycled up to 5 cycles as shown in **Figure 3.17**.

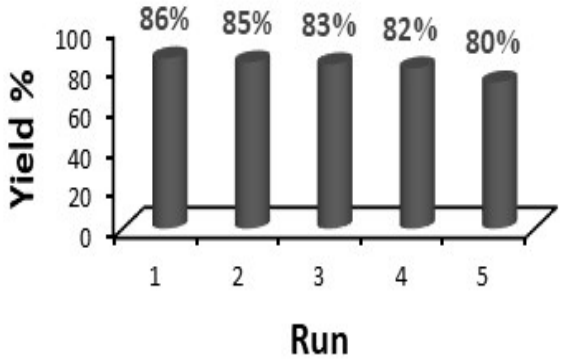

Figure 3.17 Recyclability of the catalyst **L1Ni**

3.2.4 Mechanism of C-S cross coupling reaction

To investigate the possible mechanism for this arylthiolation, a series of control reactions was carried out with *p*-tolylsulfonylhydrazide under different reaction conditions and the reaction mixtures were analyzed using mass spectroscopy (**Scheme 3.11**, steps 1 and 2). **18b** in the presence or absence of base gave only sulfinic acid **20**. When 5 mol% of **L1Ni** was added, thiosulfonate **21** (59%) was obtained together with sulfonic acid **22**, which indicates that the base has no role in the formation of **21**. Isolated **21** upon further treatment with iodobenzene under standard reaction conditions provided the desired product in 86% yield. No coupling was observed in the absence of a base, whereas the desired product was obtained when the base was present, which suggests the necessity of a base for the effective removal of halide.

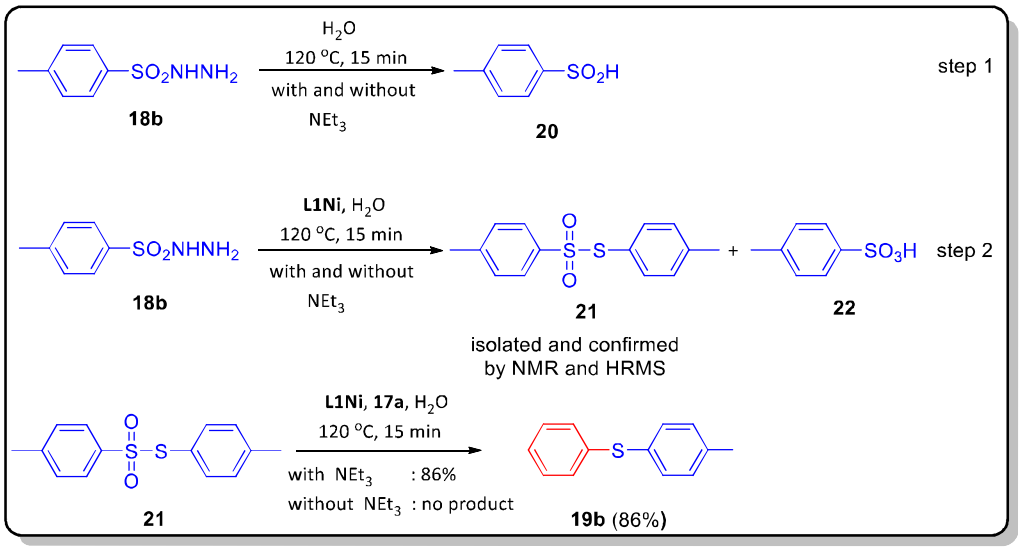

Scheme 3.11 Control experiments

Therefore, a plausible mechanistic pathway based on the above control experiments and the evidence shown in previous literature was proposed (**Scheme 3.12**) [34, 90-94]. With the aid of catalyst **L1Ni** and air oxidative decomposition, **18b** converts into sulfur source **21** with the release of N_2 and H_2O. In the catalytic cycle, the oxidative addition of the aryl halide to **L1Ni** gives nickel species **23**, which on reaction with sulfur source **21** gives nickel species **24**. Finally, upon reductive elimination, the coupling product was formed and again **L1Ni** was regenerated and used for the next catalytic cycle.

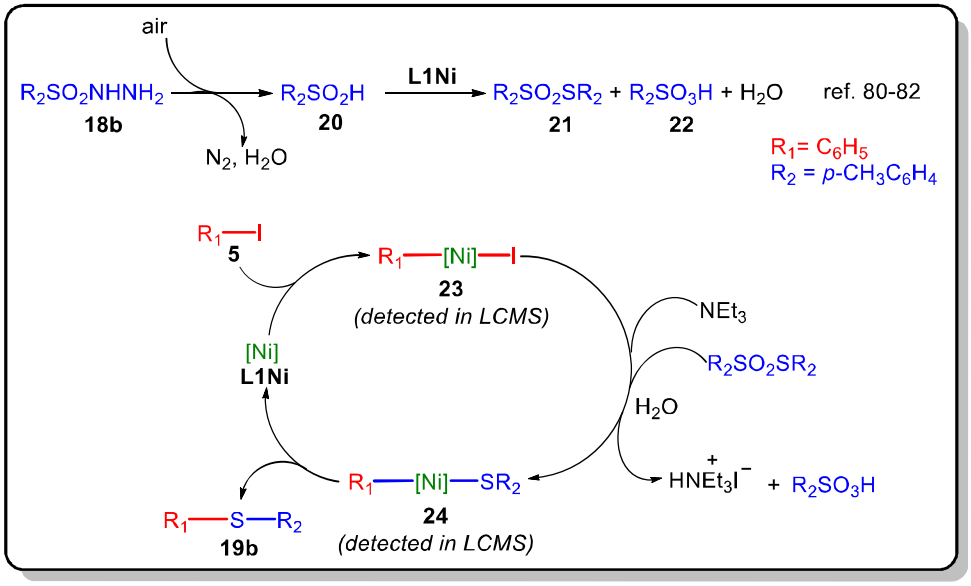

Scheme 3.12 Plausible mechanistic pathway

A few species involved in the reaction were identified with the help of mass spectrometry (**Figure 3.18-3.21**) and **21** was confirmed by ^{1}H, ^{13}C NMR (**Figure 3.22** and **Figure 3.23**) and HRMS (**Figure 3.24**).

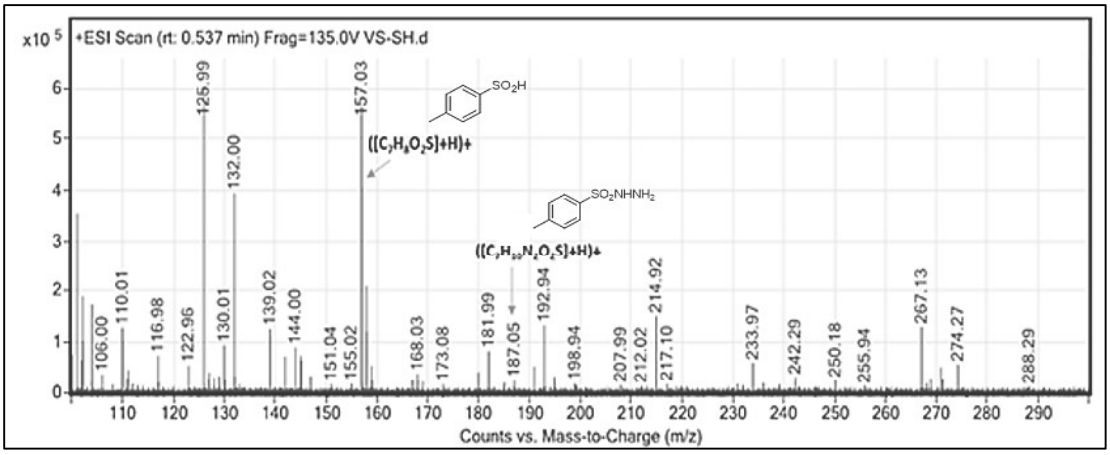

Figure 3.18 Mass spectra of reaction mixture (step 1)

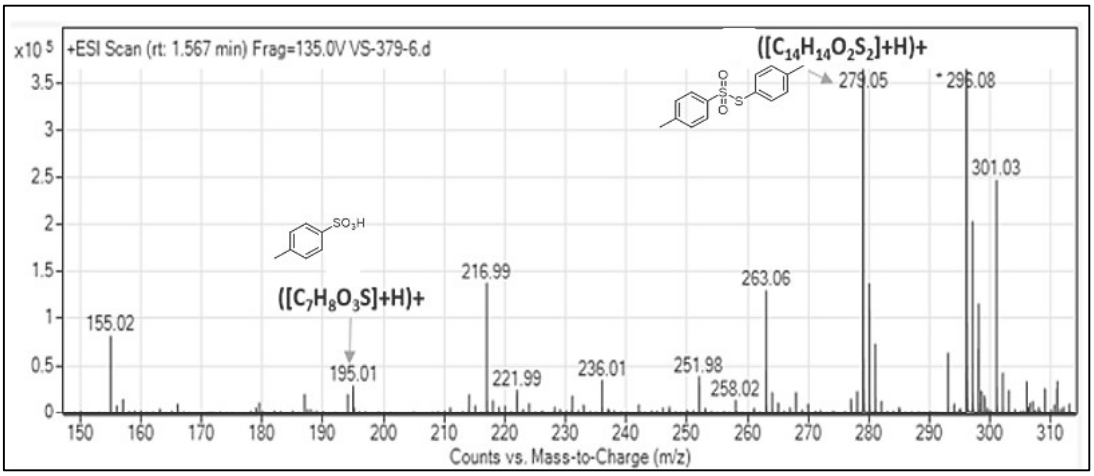

Figure 3.19 Mass spectra of reaction mixture (step 2)

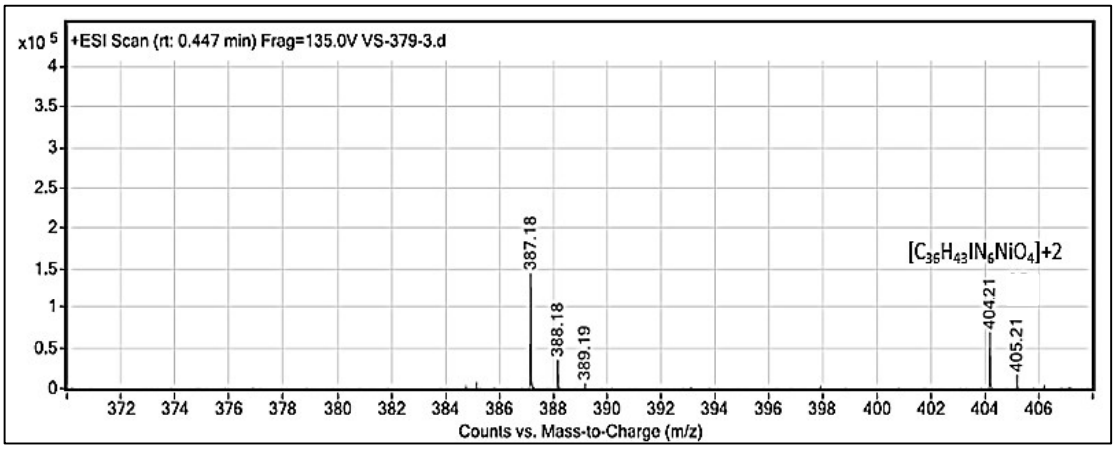

Figure 3.20 Mass spectra of species **23**

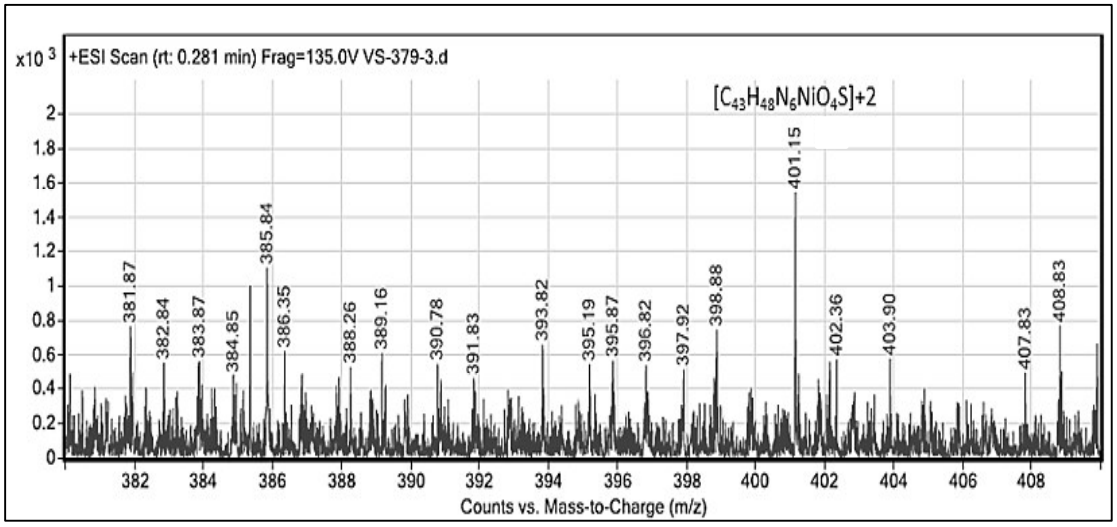

Figure 3.21 Mass spectra of species **24**

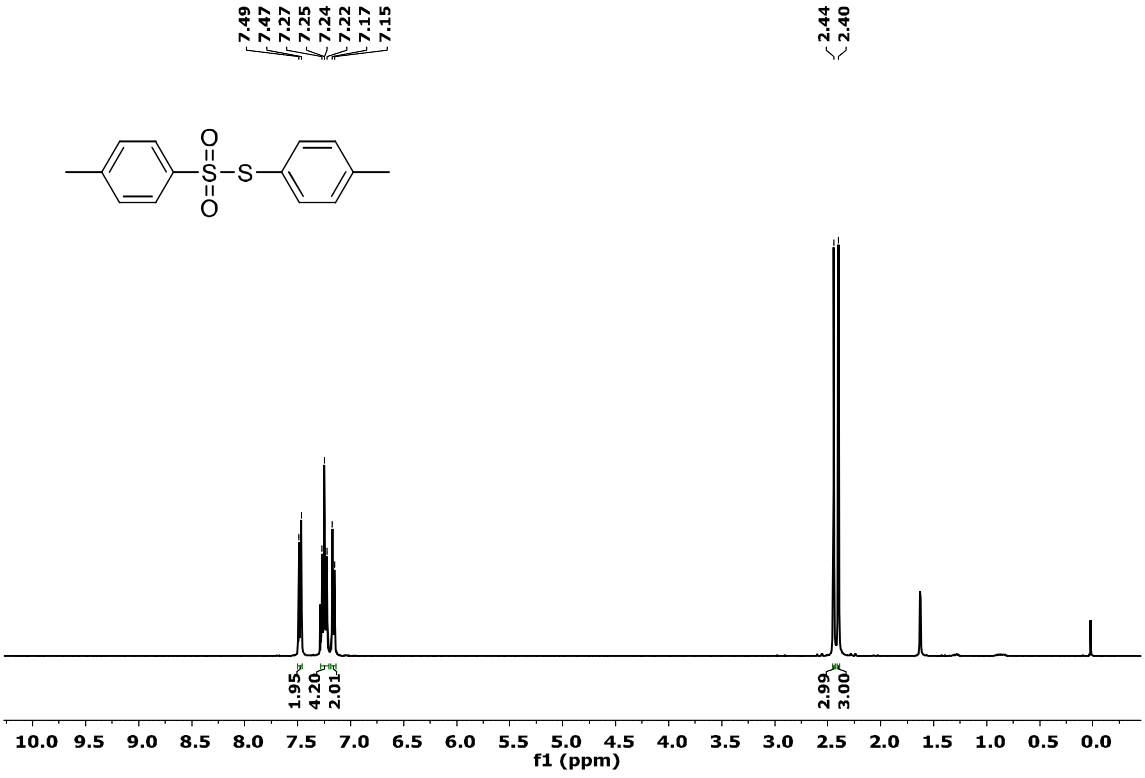

Figure 3.22 ^{1}H NMR Spectrum of isolated **21** ($CDCl_3$)

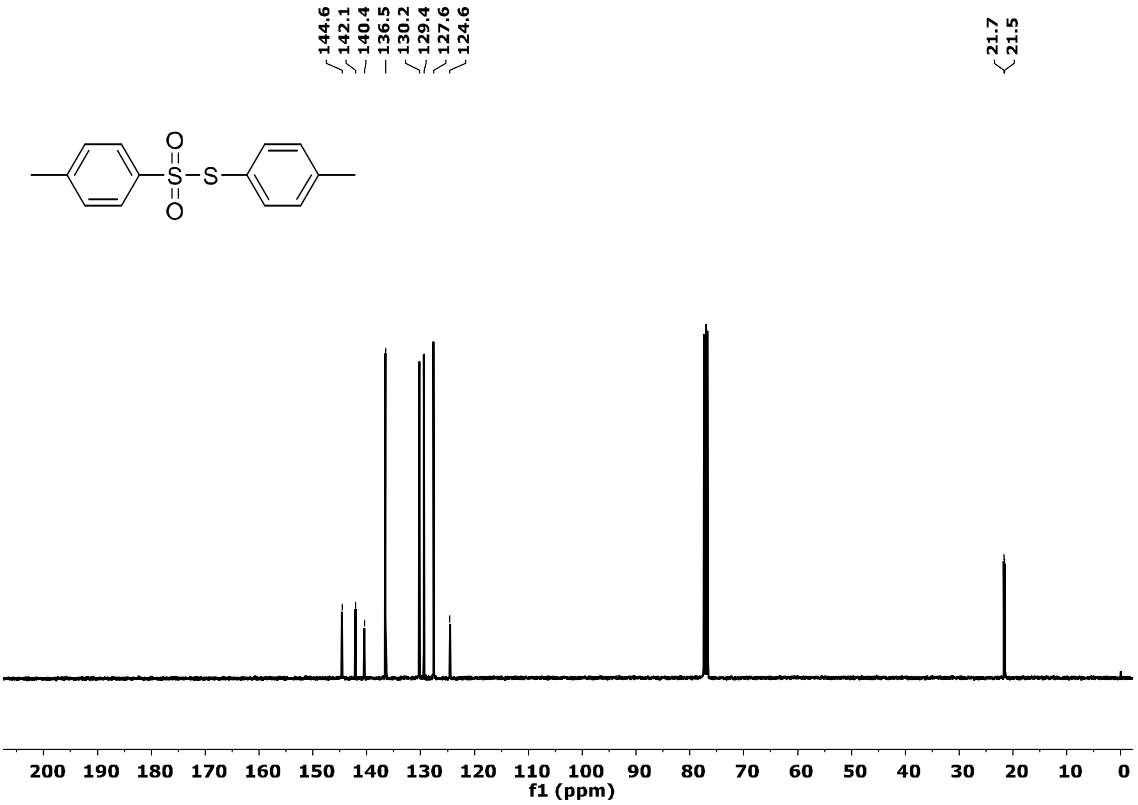

Figure 3.23 ^{13}C NMR Spectrum of isolated **21** ($CDCl_3$)

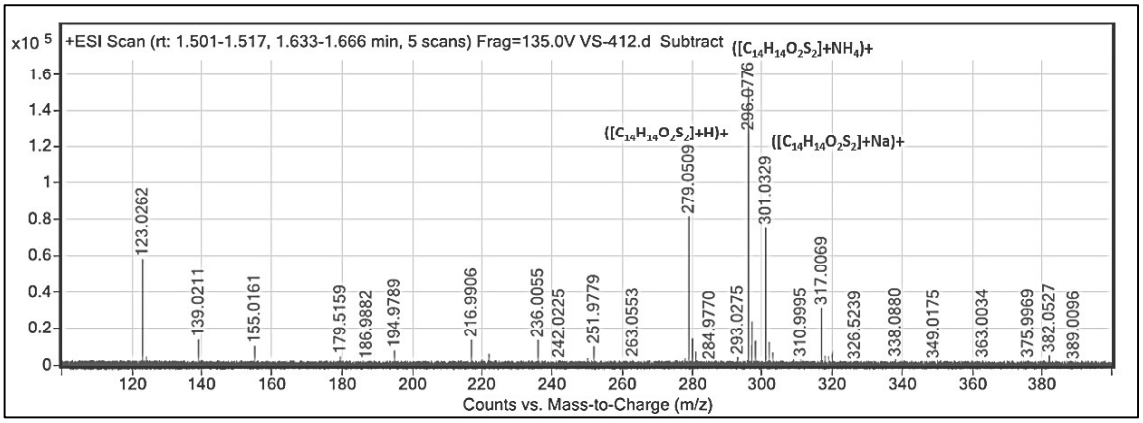

Figure 3.24 HRMS of isolated **21**

3.3 Experimental

3.3.1 Synthesis of imidazolium-based aromatic aldehyde (ImA)

A round bottom flask containing 1,3-dibromopropane (8.0 mmol), 2,4-dihydroxybenzaldehyde (6.0 mmol) and sodium bicarbonate (6.0 mmol) in acetone (50 mL)

was heated at 60 °C for 60 h. After completion, the reaction mixture was cooled down to room temperature and acetone was removed under vacuum. The residue was diluted with water and the product extracted in ethyl acetate. The ethyl acetate layer was washed with water, dried over anhydrous sodium sulfate, and evaporated under reduced pressure. The mixture was purified over a silica gel column to give pure 4-(3-bromopropoxy)-2-hydroxybenzaldehyde. A mixture of 1-methylimidazole (3.5 mmol) and 4-(3-bromopropoxy)-2-hydroxybenzaldehyde (3.5 mol) was stirred at 80 °C for 48 h to give a viscous liquid. The reaction mixture was washed with diethyl ether and ethyl acetate to give the **ImA**.

3.3.2 Synthesis of imidazolium-based salen ligand $L1H_2$

To an ethanolic solution of ethylenediamine (1 mmol), **ImA** (discussed in chapter 2, section 2.4) (1 mmol) was added dropwise. The resulting solution was refluxed for 5 h and then cooled at room temperature. The solvent was evaporated under reduced pressure and washed with ether and ethyl acetate. Obtained solid was dried under vacuum and ligand **$L1H_2$** was obtained as bright yellow solid (**Scheme 3.10**).

3.3.3 Synthesis of imidazolium-based salen nickel(II) complex L1Ni

The ligand **$L1H_2$** (1 mmol) was stirred in ethanol for 15 min. An ethanolic solution of $Ni(OAc)_2.4H_2O$ (1 mmol) was added to it and the mixture was kept on refluxing for 6 h. The resulting solution was evaporated under reduced pressure, washed with ether, ethyl acetate and after drying, **L1Ni** was isolated as a brown solid (**Scheme 3.10**).

3.3.4 General procedure for the nickel-catalyzed carbon-sulfur bond formation

A mixture of aryl iodide (1 mmol), sulfonyl hydrazide (2 mmol), NEt_3 (2 equiv.) and **L1Ni** (5 mol%) in 3 mL water was stirred under microwave irradiation at 120 °C for 15 min. After completion, the reaction mixture was cooled down to room temperature and the product extracted in ethyl acetate. The ethyl acetate layer was washed with water, dried over anhydrous sodium sulfate and evaporated under reduced pressure. The crude product was purified by column chromatography using a mixture of hexanes and ethyl acetate as the eluent.

3.3.5 Reusability and recovery of the catalyst L1Ni

After the extraction of the product, the aqueous layer containing **L1Ni** was further charged with iodobenzene, sulfonyl hydrazide, and base for the second run. The same procedure was applied for the next consecutive cycles and the catalyst was used five times.

3.3.6 Physical and spectral data of synthesized compounds

Imidazolium-based aromatic aldehyde (ImA)

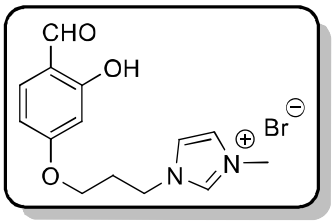

White solid (99%); mp 101-102 °C; ^{1}H NMR (400 MHz, DMSO-d_6) δ 10.02 (s, 1H), 9.25 (s, 1H), 7.84 (s, 1H), 7.74 (s, 1H), 7.62 (d, *J* = 8.64 Hz, 1H), 6.52-6.42 (m, 2H), 4.36 (t, *J* = 6.88 Hz, 2H), 4.10 (t, *J* = 5.88 Hz, 2H), 3.86 (s, 3H), 2.32-2.26 (m, 2H); ^{13}C NMR (100 MHz, DMSO-d_6) δ 193.8, 164.5, 163.8, 137.3, 134.9, 124.9, 120.2, 115.9, 109.6, 102.2, 66.7, 46.0, 36.7, 28.6.

Imidazolium-based salen ligand (L1H$_2$)

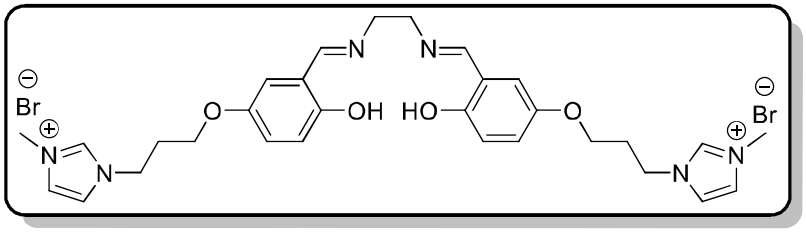

Bright yellow solid (92%); mp 130-135 °C; FTIR/cm^{-1}: 3250-3500, 1623, 1172; ^{1}H NMR (400 MHz, DMSO-d_6) δ 13.79 (s, 2H), 9.22 (s, 2H), 8.45 (s, 2H), 7.83 (s, 2H), 7.74 (s, 2H), 7.27 (d, *J* = 8.6 Hz, 2H), 6.35 (d, *J* = 2.3 Hz, 2H), 6.33 (d, *J* = 2.3 Hz, 2H), 6.29 (d, *J* = 2.2 Hz, 2H), 4.35 (t, *J* = 6.8 Hz, 4H), 4.03 (t, *J* = 5.9 Hz, 4H), 3.85 (s, 6H), 3.83 (s, 4H), 2.33-2.20 (m, 4H); ^{13}C NMR (100 MHz, DMSO-d$_6$) δ 166.1, 163.2, 161.8, 137.2, 134.3, 124.0, 122.9, 115.3, 105.5, 102.4, 64.9, 58.3, 46.9, 36.3, 29.4. HRMS (ESI): *m/z* calcd for $[C_{30}H_{38}N_6O_4]^{2+}$ [**L1H$_2$** - 2Br]$^{2+}$ 273.1472, found 273.1483.

Imidazolium-based Ni complex (L1Ni)

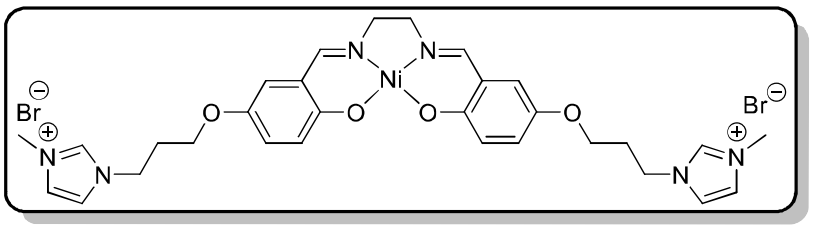

Brown solid (95%); mp 210-215 °C; FTIR/cm^{-1}: 1605, 1124; ^{1}H NMR (400 MHz, DMSO-d_6) δ 9.19 (s, 2H), 7.81 (s, 2H), 7.73 (d, *J* = 7.9 Hz, 4H), 7.16 (d, *J* = 8.7 Hz, 2H), 6.16 (s, 2H), 6.10 (d, *J* = 8.6 Hz, 2H), 4.34 (t, *J* = 6.9 Hz, 4H), 3.97 (t, *J* = 6.0 Hz, 4H), 3.85 (s, 6H), 3.33 (s, 4H), 2.41-2.16 (m, 4H); ^{13}C NMR (100 MHz, DMSO-d_6) δ 166.3, 165.8, 162.6, 137.2, 133.7, 124.0, 122.9, 112.6, 106.5, 102.0, 65.1, 57.6, 46.8, 36.2, 29.4. HRMS (ESI): *m/z* calcd for $[C_{30}H_{36}N_6O_4Ni]^{2+}$ [**L1Ni** - 2Br]$^{2+}$ 301.1071, found 301.1069.

^{1}H NMR and ^{13}C NMR Spectral data of the C-S cross-coupling products

Diphenylsulfane (19a)

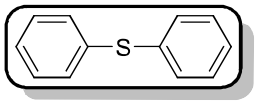

Colourless oil; ^{1}H NMR (400 MHz, $CDCl_3$) δ 7.40-7.25 (m, 10H); ^{13}C NMR (100 MHz, $CDCl_3$) δ 135.8, 131.1, 129.2, 127.0.

Phenyl(*p*-tolyl)sulfane (19b and 19b′)

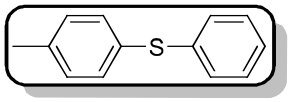

Colourless oil; ^{1}H NMR (400 MHz, $CDCl_3$) δ 7.34 (d, J = 1.9 Hz, 1H), 7.32 (d, J = 1.8 Hz, 2H), 7.30 (s, 2H), 7.24-7.21 (m, 1H), 7.19-7.15 (m, 3H), 2.37 (s, 3H); ^{13}C NMR (100 MHz, $CDCl_3$) δ 137.6, 137.1, 132.3, 131.3, 130.1, 129.8, 129.0, 126.4, 21.2.

(4-Methoxyphenyl)(phenyl)sulfane (19c)

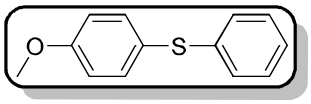

Colourless oil; ^{1}H NMR (400 MHz, $CDCl_3$) δ 7.44 (d, J = 8.8 Hz, 2H), 7.27-7.15 (m, 5H), 6.93 (d, J = 8.8 Hz, 2H), (3.85 Hz, 3H); ^{13}C NMR (100 MHz, $CDCl_3$) δ 159.8, 138.6, 135.4, 128.9, 128.2, 125.8, 124.3, 115.0, 55.4.

(4-Nitrophenyl)(phenyl)sulfane (19d and 19d′)

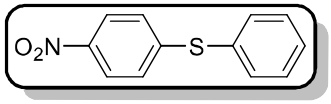

Yellow solid; ^{1}H NMR (400 MHz, $CDCl_3$) δ 8.09 (d, J = 9.1 Hz, 2H), 7.58-7.58 (m, 2.6 Hz, 2H), 7.50-7.47 (m, 2H), 7.20 (d, J = 9.1 Hz, 3H); ^{13}C NMR (100 MHz, $CDCl_3$) δ 148.5, 145.5, 134.8, 130.5, 130.1, 129.7, 126.7, 124.1.

2-Nitrophenyl phenyl sulfane (19e)

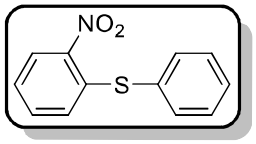

Yellow solid; ^{1}H NMR (400 MHz, $CDCl_3$) δ 8.25 (dd, J = 8.3, 1.4 Hz, 1H), 7.63-7.59 (m, 2H), 7.53-7.50 (m, 3H), 7.36 (d, J = 2.5 Hz, 1H), 7.28-7.19 (m, 1H), 6.88 (dd, J = 8.2, 1.2 Hz, 1H); ^{13}C NMR (100 MHz, $CDCl_3$) δ 144.0, 139.5, 135.9, 133.4, 131.0, 130.1, 130.0, 128.3, 125.8, 124.9.

(4-Chlorophenyl)(phenyl)sulfane (19f)

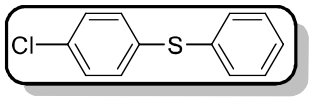

White solid; ^{1}H NMR (400 MHz, $CDCl_3$) 7.38-7.25 (m, 9H); ^{13}C NMR (100 MHz, $CDCl_3$); δ 135.1, 134.7, 133.0, 132.0, 131.3, 129.3, 127.4.

Di-(*p*-tolyl)sulfane (19g)

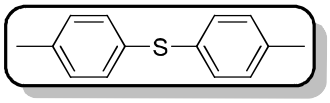

White solid; ^{1}H NMR (400 MHz, $CDCl_3$) δ 7.25 (d, J = 7.9 Hz, 4H), 7.12 (d, J = 7.9 Hz, 4H), 2.35 (s, 6H); ^{13}C NMR (100 MHz, $CDCl_3$) δ 136.9, 132.7, 131.1, 129.9, 21.1.

(4-Methoxyphenyl)(*p*-tolyl)sulfane (19h)

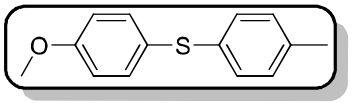

Colourless oil; ^{1}H NMR (400 MHz, DMSO) δ 7.35 (d, J = 8.8 Hz, 2H), 7.16-7.07 (m, 4H), 6.98 (d, J= 8.8 Hz, 2H), 3.77 (s, 3H), 2.26 (s, 3H); ^{13}C NMR (100 MHz, DMSO) δ 159.8, 136.4, 134.7, 134.1, 130.4, 129.4, 124.8, 115.7, 55.7, 21.0.

(4-Nitrophenyl)(*p*-tolyl)sulfane (19i and 19i′)

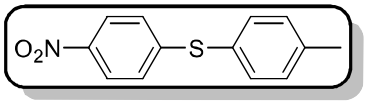

Light yellow solid; ^{1}H NMR (400 MHz, $CDCl_3$) δ 8.07 (d, J = 9.1 Hz, 2H), 7.46 (d, J = 8.2 Hz, 2H), 7.30 (d, J = 8.8 Hz, 2H), 7.15 (d, J = 8.9 Hz, 2H), 2.44 (s, 3H); ^{13}C NMR (100 MHz, $CDCl_3$) δ149.4, 145.1, 140.3, 135.1, 130.9, 126.5, 126.1, 124.0, 21.4.

(4-Chlorophenyl)(p-tolyl)sulfane (19j)

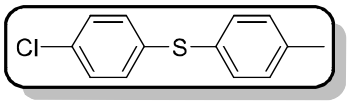

Colourless oil; ^{1}H NMR (400 MHz, $CDCl_3$) δ 7.34-7.29 (m, 4H), 7.21-7.16 (m, 4H), 2.38 (s, 3H); ^{13}C NMR (100 MHz, $CDCl_3$) δ 138.1, 136.0, 132.5, 132.3, 130.8, 130.2, 129.5, 129.1, 21.2.

4-fluorophenyl 4-nitrophenyl sulfane (19k)

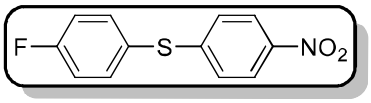

Light yellow solid; ^{1}H NMR (400 MHz, $CDCl_3$) δ 8.09 (d, J = 8.9 Hz, 2H), 7.61-7.53 (m, 2H), 7.24-7.11 (m, 4H); ^{13}C NMR (100 MHz, $CDCl_3$) δ 164.95, 162.45, 148.51, 145.38, 137.30, 137.21, 126.27, 125.48, 125.45, 124.10, 117.49, 117.27.

2-amino-4-nitrodiphenyl sulfane (19l)

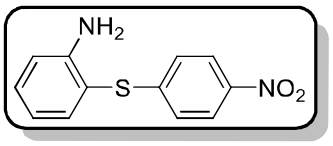

Light yellow solid; ^{1}H NMR (400 MHz, $CDCl_3$-*d*) δ 8.08 (d, J = 8.9 Hz, 1H), 7.47 (d, J = 7.6 Hz, 1H), 7.34 (d, J = 7.2 Hz, 1H), 7.13 (d, J = 8.9 Hz, 2H), 6.92-6.77 (m, 2H), 4.31 (s, 2H); ^{13}C NMR (100 MHz, $CDCl_3$) δ 148.7 , 147.8 , 139.4 , 137.3 , 130.4 , 128.4 , 124.0 , 117.9 , 115.8 , 114.8.

Benzyl(phenyl)sulfane (19m)

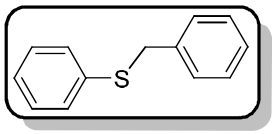

Colourless oil; ^{1}H NMR (400 MHz, $CDCl_3$) δ 7.36-7.19 (m, 10H), 4.15 (s, 2H); ^{13}C NMR (100 MHz, $CDCl_3$) δ 137.5, 136.4, 129.8, 128.9, 128.5, 127.2, 126.4, 39.1.

Benzyl(4-nitrophenyl)sulfane (19n)

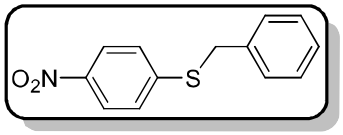

Yellow solid; ^{1}H NMR (400 MHz, $CDCl_3$) δ 8.13 (d, J = 9.0 Hz, 2H), 7.44-7.30 (m, 7H), 4.28 (s, 2H); ^{13}C NMR (100 MHz, $CDCl_3$) δ 147.2, 145.2, 135.4, 128.9, 128.7, 127.8, 126.6, 123.9, 37.0.

(4-(tert-butyl)phenyl)(phenyl)sulfane (19o)

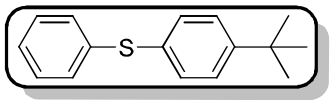

Colourless oil; ^{1}H NMR (400 MHz, $CDCl_3$) δ 7.35-7.25 (m, 9H), 1.31 (s, 9H); ^{13}C NMR (100 MHz, $CDCl_3$) δ 150.6, 136.7, 131.5, 131.1, 130.3, 129.1, 126.6, 126.3, 34.6, 31.3.

(4-(tert-Butyl)phenyl)(4-methoxyphenyl)sulfane (19p)

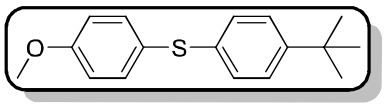

Colourless oil; ^{1}H NMR (400 MHz, $CDCl_3$) δ 7.43 (d, J = 8.9 Hz, 2H), 7.31 (d, J = 8.6 Hz, 2H), 7.17 (d, J = 8.6 Hz, 2H), 6.92 (d, J = 8.8 Hz, 2H), 3.84 (s, 3H), 1.32 (s, 9H); ^{13}C NMR (100 MHz, $CDCl_3$) δ 159.6, 149.2, 134.8, 134.7, 128.6, 126.0, 125.1, 114.9, 55.4, 34.4, 31.3.

Naphthalen-2-yl(phenyl)sulfane (19q)

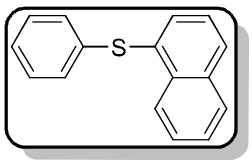

White solid; ^{1}H NMR (400 MHz, $CDCl_3$) δ 7.86 (d, J = 1.4 Hz, 1H), 7.85-7.74 (m, 3H), 7.53-7.29 (m, 8H); ^{13}C NMR (100 MHz, $CDCl_3$) δ 135.8, 133.8, 133.0, 132.3, 131.0, 129.9, 129.2, 128.9, 128.8, 127.7, 127.4, 127.1, 126.6, 126.2.

Naphthalen-2-yl(p-tolyl)sulfane (19r)

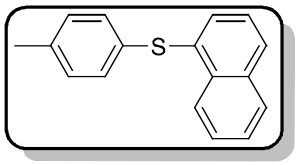

White solid; ^{1}H NMR (400 MHz, $CDCl_3$) δ 7.80-7.67 (m, 3H), 7.62 (s, 1H), 7.50-7.42 (m, 4H), 7.32 (dd, J = 8.6, 1.9 Hz, 1H), 6.94 (d, J = 8.9 Hz, 2H), 3.86 (s, 3H); ^{13}C NMR (100 MHz, $CDCl_3$) δ 159.8, 135.9, 135.2, 133.8, 131.7, 128.5, 127.7, 127.1, 126.7, 126.5, 126.5, 125.6, 124.4, 115.0, 55.4.

(4-methoxyphenyl)(naphthalen-2-yl)sulfane (19s)

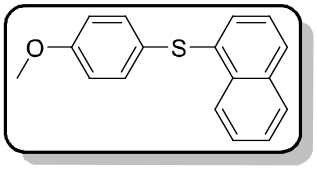

White solid; ^{1}H NMR (400 MHz, $CDCl_3$) δ 7.80-7.71 (m, 4H), 7.47-7.35 (m, 5H), 7.19 (d, J = 7.9 Hz, 2H), 2.39 (s, 3H); ^{13}C NMR (100 MHz, $CDCl_3$) δ 137.6, 134.3, 133.8, 132.1, 130.1, 128.7, 128.4, 127.9, 127.7, 127.3, 126.5, 125.9, 21.2.

4-methylbenzenesulfonothioic acid S-(4-methylphenyl) ester (21)

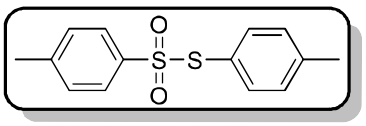

White solid; ^{1}H NMR (400 MHz, $CDCl_3$) δ 7.48 (d, J = 8.3 Hz, 2H), 7.28-7.21 (t, 4H), 7.16 (d, J = 8.0 Hz, 2H), 2.44 (s, 3H), 2.40 (s, 3H); ^{13}C NMR (100 MHz, $CDCl^3$) δ 144.6, 142.1, 140.4, 136.5, 130.2, 129.4, 127.6, 124.6, 21.7, 21.5.

3.4 Conclusion

In summary, an imidazolium-based nickel catalyst for the cross-coupling reaction of different sulfonyl hydrazides with aryl halides under microwave irradiation using water as the solvent is developed. Sulfonyl hydrazides worked well as a sulfenylating agent for C-S bond formation and afforded various symmetrical and unsymmetrical thioethers in moderate to good yields under mild reaction conditions. The reaction in water and recycling of the catalyst makes this protocol green and environmentally friendly.

3.5 References

[1] Tasker, S. Z.; Standley, E. A.; Jamison, T. F. *Nature* **2014**, *509*, 299-309.

[2] Standley, E. A.; Tasker, S. Z.; Jensen, K. L.; Jamison, T. F. *Accounts of Chemical Research* **2015**, *48*, 1503-1514.

[3] Lu, L. K.; Warshaw, E. M.; Dunnick, C. A. *Dermatologic Clinics* **2009**, *27*, 155-161.

[4] Davis, J. R., *Nickel, Cobalt, and Their Alloys*. ASM International: **2000**.

[5] P. Rothwell, I. *Chemical Communications* **1997**, 1331-1338.

[6] Yu, Z.; Hu, X.; Jia, P.; Zhang, Z.; Dong, D.; Hu, G.; Hu, S.; Wang, Y.; Xiang, J. *Applied Catalysis B: Environmental* **2018**, *237*, 538-553.

[7] Hoşgün, H. L.; Yıldız, M.; Gerçel, H. F. *Industrial & Engineering Chemistry Research* **2012**, *51*, 3863-3869.

[8] Aslam, S.; Subhan, F.; Yan, Z.; Xing, W.; Zeng, J.; Liu, Y.; Ikram, M.; Rehman, S.; Ullah, R. *Microporous and Mesoporous Materials* **2015**, *214*, 54-63.

[9] Li, C.; Kawamata, Y.; Nakamura, H.; Vantourout, J. C.; Liu, Z.; Hou, Q.; Bao, D.; Starr, J. T.; Chen, J.; Yan, M.; Baran, P. S. *Angewandte Chemie International Edition* **2017**, *56*, 13088-13093.

[10] Wang, W.; Chu, W.; Wang, N.; Yang, W.; Jiang, C. *International Journal of Hydrogen Energy* **2016**, *41*, 967-975.

[11] Zubkevich, S. V.; Tuskaev, V. A.; Gagieva, S. C.; Pavlov, A. A.; Khrustalev, V. N.; Polyakova, O. V.; Zarubin, D. N.; Kurmaev, D. A.; Kolosov, N. A.; Bulychev, B. M. *New Journal of Chemistry* **2020**, *44*, 981-993.

[12] Kinnunen, T.-J. J.; Haukka, M.; Pakkanen, T. T.; Pakkanen, T. A. *Journal of Organometallic Chemistry* **2000**, *613*, 257-262.

[13] Routaray, A.; Mantri, S.; Nath, N.; Sutar, A. K.; Maharana, T. *Polyhedron* **2016**, *119*, 335-341.

[14] Prakasham, A. P.; Ghosh, P. *Inorganica Chimica Acta* **2015**, *431*, 61-100.

[15] Standley, E. A.; Smith, S. J.; Müller, P.; Jamison, T. F. *Organometallics* **2014**, *33*, 2012-2018.

[16] Magano, J.; Monfette, S. *ACS Catalysis* **2015**, *5*, 3120-3123.

[17] Sankaralingam, M.; Balamurugan, M.; Palaniandavar, M. *Coordination Chemistry Reviews* **2020**, *403*, 213085-213099.

[18] Park, D.; Jette, C. I.; Kim, J.; Jung, W.-O.; Lee, Y.; Park, J.; Kang, S.; Han, M. S.; Stoltz, B. M.; Hong, S. *Angewandte Chemie International Edition* **2020**, *59*, 775-779.

[19] Magubane, M. N.; Nyamato, G. S.; Ojwach, S. O.; Munro, O. Q. *RSC Advances* **2016**, *6*, 65205-65221.

[20] Zheng, B.; Tang, F.; Luo, J.; Schultz, J. W.; Rath, N. P.; Mirica, L. M. *Journal of the American Chemical Society* **2014**, *136*, 6499-6504.

[21] Knappke, C. E. I.; Grupe, S.; Gärtner, D.; Corpet, M.; Gosmini, C.; Jacobi von Wangelin, A. *Chemistry A European Journal* **2014**, *20*, 6828-6842.

[22] Chauhan, P.; Mahajan, S.; Enders, D. *Chemical Reviews* **2014**, *114*, 8807-8864.

[23] Richter, M. *Natural Product Reports* **2013**, *30*, 1324-1345.

[24] Mueller, E. G. *Nature Chemical Biology* **2006**, *2*, 185-194.

[25] Lara, L. S.; Moreira, C. S.; Calvet, C. M.; Lechuga, G. C.; Souza, R. S.; Bourguignon, S. C.; Ferreira, V. F.; Rocha, D.; Pereira, M. C. S. *European Journal of Medicinal Chemistry* **2018**, *144*, 572-581.

[26] Desroches, J.; Kieffer, C.; Primas, N.; Hutter, S.; Gellis, A.; El-Kashef, H.; Rathelot,

P.; Verhaeghe, P.; Azas, N.; Vanelle, P. *European Journal of Medicinal Chemistry* **2017**, *125*, 68-86.

[27] Rajeshkumar, V.; Neelamegam, C.; Anandan, S. *Organic & Biomolecular Chemistry* **2019**, *17*, 982-991.

[28] Xu, X.-B.; Lin, Z.-H.; Liu, Y.; Guo, J.; He, Y. *Organic & Biomolecular Chemistry* **2017**, *15*, 2716-2720.

[29] Robinson, A.; Thomas, G. L.; Spandl, R. J.; Welch, M.; Spring, D. R. *Organic & Biomolecular Chemistry* **2008**, *6*, 2978-2981.

[30] Parumala, S. K. R.; Surasani, S. R.; Peddinti, R. K. *New Journal of Chemistry* **2014**, *38*, 5268-5271.

[31] Liu, G.; Huth, J. R.; Olejniczak, E. T.; Mendoza, R.; DeVries, P.; Leitza, S.; Reilly, E. B.; Okasinski, G. F.; Fesik, S. W.; von Geldern, T. W. *Journal of Medicinal Chemistry* **2001**, *44*, 1202-1210.

[32] Beletskaya, I. P.; Ananikov, V. P. *Chemical Reviews* **2011**, *111*, 1596-1636.

[33] Eichman, C. C.; Stambuli, J. P. *Molecules* **2011**, *16*, 590-608.

[34] Bour, J. R.; Camasso, N. M.; Sanford, M. S. *Journal of the American Chemical Society* **2015**, *137*, 8034-8037.

[35] Schultz, J. W.; Fuchigami, K.; Zheng, B.; Rath, N. P.; Mirica, L. M. *Journal of the American Chemical Society* **2016**, *138*, 12928-12934.

[36] Ding, L.; Zhang, Y.; Chen, X.; Lü, X. *Inorganic Chemistry Communications* **2017**, *76*, 100-102.

[37] Chatterjee, D.; Mukherjee, S.; Mitra, A. *Journal of Molecular Catalysis A: Chemical* **2000**, *154*, 5-8.

[38] Shepherd, N. E.; Tanabe, H.; Xu, Y.; Matsunaga, S.; Shibasaki, M. *Journal of the American Chemical Society* **2010**, *132*, 3666-3667.

[39] Kureshy, R. I.; Khan, N. H.; Abdi, S. H. R.; Patel, S. T.; Iyer, P.; Suresh, E.; Dastidar, P. *Journal of Molecular Catalysis A: Chemical* **2000**, *160*, 217-227.

[40] Sutradhar, M.; Roy Barman, T.; Pombeiro, A. J. L.; Martins, L. M. D. R. S. *Catalysts* **2019**, *9*.

[41] Abubakar, S.; Ibrahim, H.; Bala, M. D. *Inorganica Chimica Acta* **2019**, *484*, 276-282.

[42] Gogoi, P.; Hazarika, S.; Sarma, M. J.; Sarma, K.; Barman, P. *Tetrahedron* **2014**, *70*, 7484-7489.

[43] Baldovino-Pantaleón, O.; Hernández-Ortega, S.; Morales-Morales, D. *Inorganic*

Chemistry Communications **2005**, *8*, 955-959.

[44] Baldovino-Pantaleón, O.; Hernández-Ortega, S.; Morales-Morales, D. *Advanced Synthesis & Catalysis* **2006**, *348*, 236-242.

[45] Gómez-Benítez, V.; Baldovino-Pantaleón, O.; Herrera-Álvarez, C.; Toscano, R. A.; Morales-Morales, D. *Tetrahedron Letters* **2006**, *47*, 5059-5062.

[46] Zhang, J.; Medley, C. M.; Krause, J. A.; Guan, H. *Organometallics* **2010**, *29*, 6393-6401.

[47] Gómez-Benítez, V.; Valdés, H.; Hernández-Ortega, S.; Manuel German-Acacio, J.; Morales-Morales, D. *Polyhedron* **2018**, *143*, 144-148.

[48] Serrano-Becerra, J. M.; Valdés, H.; Canseco-González, D.; Gómez-Benítez, V.; Hernández-Ortega, S.; Morales-Morales, D. *Tetrahedron Letters* **2018**, *59*, 3377-3380.

[49] Venkanna, G. T.; Arman, H. D.; Tonzetich, Z. J. *ACS Catalysis* **2014**, *4*, 2941-2950.

[50] Basauri-Molina, M.; Hernández-Ortega, S.; Morales-Morales, D. *European Journal of Inorganic Chemistry* **2014**, *2014*, 4619-4625.

[51] Gehrtz, P. H.; Geiger, V.; Schmidt, T.; Sršan, L.; Fleischer, I. *Organic Letters* **2019**, *21*, 50-55.

[52] Zhang, Y.; Ngeow, K. C.; Ying, J. Y. *Organic Letters* **2007**, *9*, 3495-3498.

[53] Iglesias, M. J.; Prieto, A.; Nicasio, M. C. *Advanced Synthesis & Catalysis* **2010**, *352*, 1949-1954.

[54] Martin, A. R.; Nelson, D. J.; Meiries, S.; Slawin, A. M. Z.; Nolan, S. P. *European Journal of Organic Chemistry* **2014**, *2014*, 3127-3131.

[55] Junquera, L. B.; Fernández, F. E.; Puerta, M. C.; Valerga, P. *European Journal of Inorganic Chemistry* **2017**, *2017*, 2547-2556.

[56] Yoon, H.-J.; Choi, J.-W.; Kang, H.; Kang, T.; Lee, S.-M.; Jun, B.-H.; Lee, Y.-S. *Synlett* **2010**, *2010*, 2518-2522.

[57] Sikari, R.; Sinha, S.; Das, S.; Saha, A.; Chakraborty, G.; Mondal, R.; Paul, N. D. *The Journal of Organic Chemistry* **2019**, *84*, 4072-4085.

[58] Kumar, G.; Hussain, F.; Gupta, R. *Dalton Transactions* **2017**, *46*, 15023-15031.

[59] Kumar, A.; Kumar, S. *Tetrahedron* **2014**, *70*, 1763-1772.

[60] Pluta, R.; Nikolaienko, P.; Rueping, M. *Angewandte Chemie International Edition* **2014**, *53*, 1650-1653.

[61] Prokopcová, H.; Kappe, C. O. *The Journal of Organic Chemistry* **2007**, *72*, 4440-4448.

[62] Henke, A.; Srogl, J. *Chemical Communications* **2011**, *47*, 4282-4284.

[63] Taniguchi, N. *The Journal of Organic Chemistry* **2007**, *72*, 1241-1245.

[64] Savarin, C.; Srogl, J.; Liebeskind, L. S. *Organic Letters* **2002**, *4*, 4309-4312.

[65] Bakkestuen, A. K.; Gundersen, L.-L. *Tetrahedron Letters* **2003**, *44*, 3359-3362.

[66] Munday, R. *Free Radical Biology and Medicine* **1989**, *7*, 659-673.

[67] Paál, Z.; Matusek, K.; Muhler, M. *Applied Catalysis A: General* **1997**, *149*, 113-132.

[68] Lee, C.-F.; Liu, Y.-C.; Badsara, S. S. *Chemistry – An Asian Journal* **2014**, *9*, 706-722.

[69] Wang, L.; He, W.; Yu, Z. *Chemical Society Reviews* **2013**, *42*, 599-621.

[70] Li, X.; Xu, Y.; Wu, W.; Jiang, C.; Qi, C.; Jiang, H. *Chemistry A European Journal* **2014**, *20*, 7911-7915.

[71] Kumaraswamy, G.; Raju, R. *Advanced Synthesis & Catalysis* **2014**, *356*, 2591-2598.

[72] Paul, S.; Shrestha, R.; Edison, T. N. J. I.; Lee, Y. R.; Kim, S. H. *Advanced Synthesis & Catalysis* **2016**, *358*, 3050-3056.

[73] Yu, Q.; Yang, Y.; Wan, J.-P.; Liu, Y. *The Journal of Organic Chemistry* **2018**, *83*, 11385-11391.

[74] Singh, N.; Singh, R.; Raghuvanshi, D. S.; Singh, K. N. *Organic Letters* **2013**, *15*, 5874-5877.

[75] Singh, R.; Allam, B. K.; Singh, N.; Kumari, K.; Singh, S. K.; Singh, K. N. *Advanced Synthesis & Catalysis* **2015**, *357*, 1181-1186.

[76] Wang, T.-T.; Yang, F.-L.; Tian, S.-K. *Advanced Synthesis & Catalysis* **2015**, *357*, 928-932.

[77] Sun, J.; Wang, Y.; Pan, Y. *Organic & Biomolecular Chemistry* **2015**, *13*, 3878-3881.

[78] Xu, Z.-Q.; Zheng, L.-C.; Li, L.; Duan, L.; Li, Y.-M. *Tetrahedron* **2019**, *75*, 643-651.

[79] Nookaraju, U.; Begari, E.; Yetra, R. R.; Kumar, P. *ChemistrySelect* **2016**, *1*, 81-85.

[80] Hooshmand, S. E.; Heidari, B.; Sedghi, R.; Varma, R. S. *Green Chemistry* **2019**, *21*, 381-405.

[81] Rathi, A. K.; Gawande, M. B.; Zboril, R.; Varma, R. S. *Coordination Chemistry Reviews* **2015**, *291*, 68-94.

[82] Khungar, B.; Rao, M. S.; Pericherla, K.; Nehra, P.; Jain, N.; Panwar, J.; Kumar, A. *Comptes Rendus Chimie* **2012**, *15*, 669-674.

[83] Nehra, P.; Khungar, B.; Pericherla, K.; Sivasubramanian, S. C.; Kumar, A. *Green Chemistry* **2014**, *16*, 4266-4271.

[84] Faniran, J. A.; Patel, K. S.; Bailar, J. C. *Journal of Inorganic and Nuclear Chemistry* **1974**, *36*, 1547-1551.

[85] Ueno, K.; Martell, A. E. *The Journal of Physical Chemistry* **1956**, *60*, 1270-1275.

[86] Rajasekar, M.; Sreedaran, S.; Prabu, R.; Narayanan, V.; Jegadeesh, R.; Raaman, N.; Kalilur Rahiman, A. *Journal of Coordination Chemistry* **2010**, *63*, 136-146.

[87] Santos, I. C.; Vilas-Boas, M.; Piedade, M. F. M.; Freire, C.; Duarte, M. T.; de Castro, B. *Polyhedron* **2000**, *19*, 655-664.

[88] Abdel Aziz, A. A.; Badr, I. H. A.; El-Sayed, I. S. A. *Spectrochimica Acta Part A: Molecular and Biomolecular Spectroscopy* **2012**, *97*, 388-396.

[89] Naik, A. D.; Fontaine, G.; Bellayer, S.; Bourbigot, S. *RSC Advances* **2015**, *5*, 48224-48235.

[90] Deavin, A.; Rees, C. W. *Journal of the Chemical Society (Resumed)* **1961**, 4970-4973.

[91] Kice, J. L.; Bowers, K. W. *Journal of the American Chemical Society* **1962**, *84*, 605-610.

[92] Xianwei, L.; Yanli, X.; Wanqing, W.; Chang, J.; Chaorong, Q.; Huanfeng, J. *Chemistry A European Journal* **2014**, *20*, 7911-7915.

[93] Xavier, M.; Marc, C. J.; Gilbert, M.; Anny, J. *European Journal of Organic Chemistry* **2005**, *2005*, 3749-3760.

[94] Kice, J. L.; Parham, F. M. *Journal of the American Chemical Society* **1960**, *82*, 6168-6175.